Russian Chemical Reviews **75** (7) 601 – 616 (2006) © 2006 Russian Academy of Sciences and Turpion Ltd

DOI 10.1070/RC2006v075n07ABEH003613

Features of solid-phase transformations induced by shock compression

S S Batsanov

Contents

I.	Introduction	601
II.	Shock waves	601
III.	Features of phase transitions in shock waves	607
IV.	Duration of solid-phase chemical reactions	609
V.	Mechanism of ultrafast solid-phase reaction	613
VI.	Conclusion	614

Abstract. The results of physicochemical studies of solid-phase transformations under shock compression are analysed. The characteristic time of phase transitions and chemical reactions in shock-compressed solids found experimentally does not exceed one microsecond. Possible reasons for ultrafast atom diffusion are discussed. Hydrodynamic mixing of reactants is believed to be the most feasible mechanism. Prospects for basic and applied research in the field are outlined. The bibliography includes 151 references.

I. Introduction

In synthetic chemistry, the composition and structure of compounds are often varied using high temperature and high pressure techniques. The results obtained are strongly dependent on the level of thermodynamic parameters used. While the range of appropriate high temperatures is limited by the melting or evaporation of a chemical compound, the static pressure is limited by the ultimate strength of the anvil material. Experiments with diamonds made is possible to reach a pressure of up to $\sim 10^6$ atm (~ 100 GPa) paying for an enhanced pressure with progressive diminution of the working volume (to a few micrometres). Such experiments provide new scientific information but not novel materials.

There is also a basically different method of producing high pressures, which is free from this drawback. The technique is called pulse compression of matter using shock waves, or simply shock compression. Physics of pulse pressures rapidly developed during and immediately after the World War II. The shock wave chemistry, as a new avenue of scientific research, emerged in the late 1950s and its development is to a great extent due to achievements in physics and technology of ultrafast methods of investigation. Of particular interest are investigations of the duration and mechanisms of solid-phase transformations induced or assisted by shock waves. This is the subject of the present review, which also concerns the latest advances in shock wave chemistry.

S S Batsanov Centre of High Dynamic Pressures, All-Russian Scientific Research Institute of Physical-Technical and Radiotechnical Measurements, 141570 Mendeleevo, Moscow Region, Russian Federation. Fax (7-495) 744 81 81, tel. (7-495) 535 92 88, e-mail: batsanov@gol.ru

Received 6 February 2006
Uspekhi Khimii **75** (7) 669 – 686 (2006); translated by A M Raevskiy

II. Shock waves

1. Introduction to physics of shock waves

A shock wave is a narrow region of compressed matter, which propagates with a supersonic speed. It emerges upon detonation of explosives, collisions between rapidly moving bodies and obstacles, high-power electric discharges and laser ablation of crystals (see references cited in Ref. 1).

If the shock wave is represented as a plane separating the initial and perturbed state of matter, the following equations hold on both sides of the plane in accord with the laws of mass, momentum and energy conservation:

$$\rho_0 D = \rho\,(D-U), \tag{1}$$

$$P - P_0 = \rho_0 D U, \tag{2}$$

$$\left[(E - E_0) - \frac{U^2}{2}\right]\rho_0 D = P_0 U, \tag{3}$$

where ρ is the density of matter, D is the shock-wave velocity, U is the mass (particle) velocity behind the shock wave front, P is the pressure, E is the internal energy; the subscript 'zero' corresponds to the initial state (the shock wave and particle velocities are also denoted as U_s and U_p, respectively). The state of matter under shock compression is described by the shock adiabat (or Hugoniot adiabat), most often in the $P-V$ or $D-U$ coordinates. If ρ is expressed in g cm^{-3} and the parameters D and U are expressed in km s^{-1}, the pressure P is given in GPa.

It was experimentally established that at pressures below 100 GPa the shock adiabats of many materials obey a linear relation

$$D = c_0 + \lambda U, \tag{4}$$

where c_0 is a parameter similar to the bulk sound velocity and λ is a coefficient, which characterises the slope of the shock adiabat and is of the order of unity

$$\lambda = \frac{D - c_0}{U}. \tag{5}$$

Rodean [2] proposed a relation between the coefficients c_0 and λ

$$\frac{1}{2}\left(\frac{c_0}{\lambda}\right)^2 = \Delta H_s, \tag{6}$$

where ΔH_s is the heat of sublimation (here, the heat of atomisation) of a solid. It is valid for metals and some crystalline compounds (alkali metal halides and MgO).

Relation (4) can be derived theoretically from the equation of state for internal energy of shock compression. Using the Morse function (known in spectroscopy), the following expressions for the coefficients c_0 and λ were obtained [3]

$$c_0 = \frac{A}{3B},$$

$$\lambda = \frac{A}{4} - \frac{1}{5},$$

where $A = \alpha r_0$ (α is the thermal expansion coefficient, r_0 is the bond length under normal pressure) and $B = \sqrt{E/2}$ (here E is the bond dissociation energy). Equation (4) with these coefficients quite correctly reproduces the experimental shock adiabats of metals and covalently bonded compounds. In principle, relation (4) can also be derived from other equations of state, *e.g.*, the Birch – Murnaghan and Mie – Grüneisen equations.

Large deviations of the $D = f(U)$ function from linear law are due to physicochemical transformations of compounds under shock compression and, hence, can serve as indicators of such transformations. From Eqn (5) it follows that a change in c_0 will cause antiparallel changes in the λ coefficient, namely, an increase in the sound velocity (at the same parameters D and U) leads to decrease in the slope of the Hugoniot adiabat and *vice versa*. For instance, for three forms of SiO_2 (glass, crystalline quartz and stishovite) the c_0 values are respectively equal to 1.52, 2.20 and 5.07 and λ = 1.74, 1.60 and 0.18 (see Ref. 4). Analogously, the Hugoniot equations for molybdenum [5] at room temperature and at 1400 °C, respectively, have the form

$$D = 5.136 + 1.220\,U,$$

$$D = 4.78 + 1.42\,U.$$

If Eqn (4) fails to correctly describe experimental data, a parabolic equation

$$D = c_0 + \lambda U \pm \mu U^2, \tag{7}$$

with the coefficient $\mu \ll 1$ is used. The generalised shock adiabat equation is as follows [6]

$$D = c_0 + \lambda U + \frac{\mu U^2}{c_0}. \tag{8}$$

For alkali metals, λ = 1.1 and μ = 0.04; for other metals and inorganic salts, λ = 1.5 and $\mu = -0.05$ and for organic liquids λ = 2.0 and $\mu = -0.1$. Methane, solid and liquid CO_2 and water obey the same generalised shock adiabat equation:[7]

$$D = c_0 + 1.9\,U - \frac{0.08U^2}{c_0},$$

where c_0 = 1.15, 1.8, 1.0 and 1.95, respectively.

It should be emphasised that the shock adiabat describes the bulk compression of a body. Initially, the action of dynamic pressure causes elastic compression of a crystal, which is followed by elastoplastic and then bulk compression of the body with an increase in pressure (Fig. 1). Therefore, the shock adiabat begins with a particular non-zero pressure (ponit *1*). At pressures below the pressure corresponding to point *1*, the parameters of state are usually obtained by extrapolating experimental data from the bulk compression region to $P = 0$. X-Ray diffraction studies of crystals undergoing shock compression showed that at low shock velocities a single crystal experiences uniaxial compression accompanied by a change in symmetry (*e.g.*, a cubic unit cell is transformed into a tetragonal one) while bulk compression of the body with preservation of initial symmetry occurs at high shock velocities.[8–12]

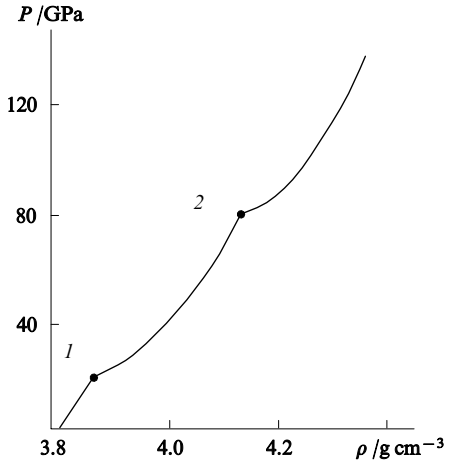


Figure 1. Shock compression diagram of a solid (Al_2O_3 single crystal). Point (*1*) corresponds to HEL pressure of 20 GPa, and point (*2*), to a phase transition at 80 GPa. Elastic compression region ($0 < P < 20$ GPa) and bulk compression region ($P > 20$ GPa).

In studies of monolithic bodies it is possible to measure their dynamic elastic limit (Hugoniot elastic limit, HEL). Experimental P_{HEL} values for the polycrystalline state of some elements are listed in Table 1. There are several elements with known P_{HEL} values; therefore, elaboration of methods of *a priori* estimation of these characteristics is required.

Based on the assumption of similarity between the plastic and liquid states of the body, the work of plastic deformation (taken with some coefficient) was equated [13] to the heat of melting, and an equation relating the HEL pressure to the change in the volume of the body upon 'mechanical melting' was derived:

$$P_{HEL} = k\frac{\Delta H_m}{\Delta V_m}, \tag{9}$$

where ΔH_m is the heat of melting, ΔV_m is the decrease in the volume of the body from the initial volume V_0 to the volume upon mechanical melting, V_m. The calculated P_{HEL} values for a number of elements with presently unknown experimental data are also listed in Table 1.

Table 1. HEL pressures (P_{HEL} /GPa) for chemical elements.[13, 14]

Experiment				Calculations	
element	P_{HEL}	element	P_{HEL}	element	P_{HEL}
Al	0.54	Mo	1.6	B	9.70
Be	0.14 – 0.55	Nb	2.07	Cd	0.20
Bi	0.3	Ni	1.0	La	0.05
C	63	Pb [a]	0	Pt	2.18
Cr	1.6	Sb	0.95	Re	4.68
Cu	0.15 – 0.63	Si	6.5	Sc	0.22
Ge	5.05	Ta	2.3 – 2.8	Tl	0.19
Fe	1.1 – 1.5	Th	0.14	Zn	0.33
Mg	0.11	Ti	1.85	Zr	0.60
		W	3.2 – 3.9		

[a] Annealed sample.

Parameters of Eqn (4) are related to the mechanical characteristics of the body measured under static loading, namely, the isentropic bulk elastic modulus (B_0) and its pressure derivative, by the following equations:[15]

$$c_0 = \sqrt{\frac{B_0}{\rho}}, \qquad (10)$$

$$\lambda = \frac{B_0' + 1}{4}.$$

These expressions make it possible to relate the parameter λ to the Grüneisen constant (Γ)

$$\Gamma = \frac{1}{c_V \sigma}\beta V_0 = \frac{1}{c_P}\beta B_0 V_0,$$

where c_V and c_P is the heat capacity at constant volume and pressure, respectively; σ is the isothermal compressibility and β is the bulk thermal expansion coefficient.

The following empirical relationship [16] correctly reproduces the experimental data for metals:

$$\beta = \frac{1}{3}\frac{B_0' + 1}{B_0 V_0} c_P. \qquad (11)$$

From this equation one gets

$$\lambda = \frac{3}{4}\Gamma. \qquad (12)$$

A number of equations describing the dependence of λ on Γ are also available. For instance, the coefficient λ is often estimated using the following relation [17]

$$\lambda = \frac{1 + \Gamma}{2}. \qquad (13)$$

When applied to metals, Eqns (12) and (13) give similar results.

As a rule, Γ is assumed to be inversely proportional to the volume of the body

$$\Gamma V = \Gamma_0 V_0.$$

However, this is not always true. For instance, in the case of NaCl an increase in pressure from 0 to 3 GPa is accompanied by reduction of the volume and a decrease in the Grüneisen constant of the material from 1.52 to 1.40 (see Ref. 18), whereas heating of molybdenum to 1400 °C leaves the Γ value unchanged (1.52).[5]

All experimentally determined coefficients in the Hugoniot equations for elements and inorganic compounds available at the moment (data taken from monograph [4] or from more recent studies cited in this review), as well as those calculated using expressions (10) are listed in Tables 2–4. All these data refer to low-pressure phases. In most cases the experimental and calcu-

Table 2. Coefficients in the Hugoniot equations of chemical elements.[4]

Element	c_0	λ	Element	c_0	λ	Element	c_0	λ	Element	c_0	λ
Li	4.760 4.659	1.065 1.15	Ge	3.151 3.77	1.79 1.375	Sb	1.98 2.429	1.63 1.525	Tc	– 4.97	– –
Na	2.624 2.585	1.188 1.225	Sn	2.437 2.727	1.688 1.55	Bi	1.861 1.795	1.520 1.675	Re	4.068 4.18	1.375 1.60
K	1.991 1.932	1.17 1.25	Pb	1.981 1.967	1.603 1.60	V	5.050 5.13	1.227 1.325	Fe	4.63 4.647	1.33 1.775
Rb	1.232 1.304	1.184 1.225	Ti	4.937 4.827	1.04 1.35	Nb	4.472 4.46	1.114 1.475	Co	4.743 4.747	1.227 1.15
Cs	0.363 0.972	1.583 1.20	Zr	3.812 3.70	0.977 1.20	Ta	3.431 3.42	1.159 1.10	Ni	4.501 4.530	1.627 1.55
Cu	3.899 3.986	1.520 1.55	Hf	2.954 2.87	1.121 1.25	O	2.327 1.20	1.215 1.35	Ru	– 5.055	– 1.90
Ag	3.178 3.177	1.773 1.675	B	– 9.06	– 1.075	S	2.334 2.13	1.588 1.75	Rh	4.775 4.639	1.331 1.375
Au	3.063 2.979	1.563 1.75	Al	5.333 5.278	1.356 1.45	Se	– 1.87	– 0.925	Pd	3.955 3.911	1.701 1.85
Be	7.993 8.030	1.132 1.10	Ga	2.501 3.144	1.560 1.00	Te	3.242 1.83	0.888 1.575	Os	– 4.170	– 1.375
Mg	4.540 4.489	1.238 1.30	In	2.560 2.401	1.477 1.65	Cr	5.153 5.00	1.557 1.55	Ir	3.930 4.015	1.536 1.45
Ca	3.438 3.397	0.968 1.05	Tl	1.809 1.721	1.597 1.575	Mo	5.100 5.11	1.266 1.30	Pt	3.605 3.614	1.560 1.575
Sr	2.10 2.128	0.94 0.975	Sc	4.496 4.48	0.955 0.95	W	4.015 4.09	1.252 1.20	He	0.712 0.761	1.36 1.35
Ba	1.108 1.603	1.369 0.90	Y	3.381 3.00	0.725 0.85	H	– 1.37	– 2.075	Ne	– 0.895	– 2.55
Zn	3.031 2.80	1.608 1.775	La	2.064 1.915	1.012 1.225	F	– 2.18	– 1.35	Ar	1.249 1.02	1.588 1.375
Cd	2.434 2.22	1.759 1.90	N	1.572 1.246	1.365 1.225	Cl	– 2.53	– 1.55	Kr	0.70 0.84	1.72 1.30
Hg	1.75 1.58	1.72 1.85	P	– 3.584	– 1.575	Br	1.51 1.88	1.24 1.55	Xe	1.16 0.815	1.40 1.40
C	12.16 11.39	1.00 1.20	As	– 3.195	– 1.325	I	1.50 1.71	1.46 1.55	Th	2.18 2.26	1.24 1.40
Si	7.99 6.48 (see [a])	1.42 1.275 (see [a])				Mn	– 4.185	– 1.70	U	2.51 2.43	1.51 1.75

Note. Here and in Tables 3 and 4 the values of the parameter c_0 are given in km s^{-1}; figures in the numerator denote experimental data and figures in denominator denote theoretical data. [a] Data taken from Ref. 19.

Table 3. Coefficients in the Hugoniot equations of low-pressure phases of metal and NH_4 halides.[4]

Cation	Fluorides		Chlorides		Bromides		Iodides	
	c_0	λ	c_0	λ	c_0	λ	c_0	λ
Li	5.15	1.35	3.93	1.41	2.92	1.33	2.87	0.89
	5.26	1.55	3.96	1.50	2.67	1.65	2.17	1.75
Na	4.25	1.36	3.385	1.38	2.62	1.32	2.09	1.576
	4.15	1.52	3.415	1.55	2.555	1.55	2.12	1.575
K	2.324	1.65	2.15	1.54	1.93	1.44	1.787	1.372
	3.55	1.55	3.02	1.60	2.40	1.60	1.97	1.60
Rb	2.067	1.419	1.565	1.615	1.585	1.47	1.337	1.518
	2.72	1.62	2.44	1.60	2.05	1.60	1.78	1.575
Cs	1.63	1.68	2.182	1.481	2.06	1.36	1.85	1.33
	2.31	–	2.133	1.60	1.88	1.60	1.64	1.65
Cu			3.08	0.21	–	–	2.50	0.43
			3.08	1.27	2.74	1.25	2.50	1.25
Ag	–	–	–	–	–	–	–	–
	2.93	–	2.81	1.85	2.505	1.95	2.02	1.09
Tl	–	–	1.85	1.54	–	–	1.35	1.56
	1.49	1.30	1.83	1.575	1.69	1.60	1.55	1.62
NH_4	–	–	3.59	1.404	–	–	–	–
	–	–	3.92	1.575	2.89	1.425	2.43	1.3

Table 4. Experimentally determined coefficients in the Hugoniot equations of low-pressure oxide, chalcogenide, nitride and carbide phases.

Phase	c_0	λ	Phase	c_0	λ
BeO	8.44	1.22	TiO_2	2.926	1.865
MgO	6.60	1.37	ZrO_2	4.38	1.37
CaO	3.80	1.59	SiO_2 (see [f])	2.20	1.596
MnO (see [a])	5.32	1.18	SiO_2 (see [g])	5.07	0.183
FeO	3.72	1.59	SiO_2 (see [h])	1.52	1.74
NiO (see [b])	5.35	1.21	GeO_2 (see [i])	5.23	1.96
ZnS	3.13	1.30	GeO_2 (see [j])	0.63	1.84
ZnSe	4.00	1.15	MnO_2	3.632	1.52
SnS	2.370	1.156	UO_2	3.88	1.11
SnTe	2.474	1.468	TiB_2 (see [k])	8.622	0.795
FeS	2.886	1.603	MgF_2	3.50	1.56
TiC	5.17	1.42	CaF_2	4.76	1.30
HfC	5.11	1.53	$Mg(OH)_2$	4.75	1.27
SiC	8.00	0.98	FeOOH	4.47	1.60
NbC	5.38	1.46	FeS_2	5.15	1.52
TaC	3.32	1.49	Fe_2O_3	6.24	1.39
WC	5.63	1.16	Fe_3O_4	4.26	1.37
BN (see [c])	7.48	1.47	Fe_3C	4.60	1.87
AlN (see [d])	3.27	1.81	Al_2O_3	7.93	1.50
TiAl (see [e])	4.36	2.92	Si_3N_4 (see [l])	4.585	1.489

[a] Data taken from Ref. 20. [b] Data taken from Ref. 21. [c] Data taken from Ref. 22. [d] For NaCl-type structure.[23] [e] Data taken from Ref. 24. [f] Quartz. [g] Stishovite. [h] Glass. [i] Rutile-type structure. [j] Quartz-type structure. [k] Data taken from Ref. 25. [l] Data taken from Ref. 26.

lated values are similar. Differences between them are due to the phase transformations at elevated pressures (as a result, the characteristics determined under shock compression correspond to certain phases that differ from the phases for which the B_0 and B_0' were measured; this is the case for, *e.g.*, tellurium).

Table 5 presents the coefficients in the Hugoniot equations of low-molecular-mass compounds and polymers obtained from Refs 4, 27 – 30 or calculated by the least squares method from experimental D and U values reported in the same studies.

Table 5. Coefficients in the Hugoniot equations of the low-pressure phases of low-molecular-mass compounds and polymers.

Compound	c [a]	λ	Compound	c [a]	λ
N_2	1.59	1.36	$(C_2H_5)_2O$	1.67	1.455
NH_3	2.00	1.51	$CHBr_3$	1.265	1.533
H_2O	1.50	2.00	C_2H_5Br	1.58	1.36
CO	1.54	1.40	$C_2H_2Cl_2$	1.11	1.75
CO_2	2.16	1.465	CH_2Br_2	1.0	1.6
CS_2	1.64	1.46	CH_2I_2	0.96	1.54
CCl_4	1.47	1.57	formic acid	1.982	1.406
CH_4 (115 K)	2.841	1.168	acetic acid	2.299	1.267
C_6H_{14}	1.738	1.446	butyric acid	2.128	1.384
C_7H_{16}	1.808	1.450	aniline	2.506	1.275
$C_{10}H_{22}$	1.970	1.458	anthracene	3.21	1.445
$C_{13}H_{28}$	2.013	1.460	phenanthrene	3.097	1.417
$C_{14}H_{30}$	2.095	1.463	pyrene	3.031	1.457
$C_{16}H_{34}$	2.127	1.464	polystyrene	2.48	1.63
C_6H_6	1.88	1.58	polyethylene (ρ = 0.92)	2.83	1.408
$C_6H_5CH_3$	1.72	1.66	polypropylene	3.00	1.42
$C_6H_5NO_2$	2.01	1.59	polyurethane	2.24	1.71
$C_6H_3(NO_2)_3$	2.318	2.025	paraffin	2.960	1.531
$C_6H_2CH_3(NO_2)_3$	2.390	2.050	plexiglass (ρ = 1.18)	3.08	1.308
CH_3NO_3	2.07	1.34	teflon (ρ = 2.18)	2.18	1.580
CH_3OH	1.73	1.50	nylon	2.500	1.747
C_2H_5OH	1.785	1.575	rubber	1.84	1.44
C_4H_9H	1.868	1.497	foam plastic		
$C_5H_{11}H$	1.988	1.487	ρ = 0.30	0.15	1.290
$C_6H_{13}H$	2.324	1.378	ρ = 0.65	1.07	1.340
$C_3H_5(OH)_3$	3.07	1.34	ρ = 0.70	1.19	1.350
$CO(CH_3)_2$	1.91	1.38	acetonitrile	2.754	1.088

[a] Coefficient c (km s^{-1}) can be significantly different from c_0.

Since the bulk and elastic compression of a body differ by

$$\Delta = D - c_0,$$

the coefficient λ depends on the compressibility of the material. For instance, based on the λ values listed in Table 2, metals can be divided into two groups. One group comprises the main-group elements (except for Cr and Group VIII metals) characterised by $\bar{\lambda} = 1.12 \pm 13\%$; while the other group comprises transition metals with $\bar{\lambda} = 1.61 \pm 7\%$. The difference is due to lower compressibility of the d-metals compared to the s,p-elements. Caesium (λ = 1.58) presents a particular case, which is probably due to physicochemical transformations of this metal (oxidation or phase transitions) in the course of sample preparation or during the shock compression experiments.

The aforesaid concerns monolithic bodies. However chemists most often work with powders. Here, the porosity of the materials should be taken into account. Propagation of a shock wave through a porous material is accompanied by the 'collapse' of pores and compaction of the powder to form a monolithic body, friction of particles during compaction, their grinding due to unloading (expansion) of the hard material to a softer one or to a pore, deformation of crystalline grains and plastic flow, which leads to heat release and possible contact melting of particles. Highly porous materials are heated to so high temperatures that the effect of heating can exceed the effect of the high pressure (anomalous compression) (Fig. 2).[31] Shock compression of porous materials with very high porosities made it possible to obtain dense high-temperature plasma.[32 – 34]

A number of models are available, in which porous materials under shock compression are treated as loose monolithic bodies (a review of such models can be found in Ref. 35). The Hugoniot adiabats of powders are also calculated under assumption of heterogeneous medium ('mixture of monolithic body and air'). The following equation was derived[6] assuming a seven-fold decrease in the pore volume upon compression

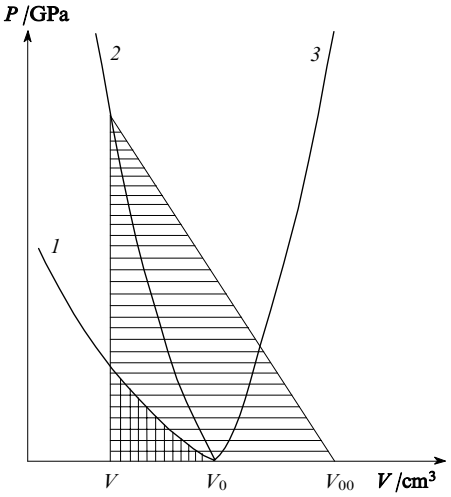


Figure 2. Shock compression diagrams of bodies of different porosity. Monolithic body ($V_0 \to V$) (*1*), porous body ($V_{00} \to V$) (*2*), anomalous compressibility of highly porous material (starting point is shifted towards V_0) (*3*); regions filled with horizontal lines and squares correspond to the energies of compression of porous and monolithic bodies, respectively; V is the final volume of compressed body, V_0 is the volume of monolithic body and V_{00} is the powder volume.

$$U_*^2 = U^2 + \frac{6}{7}(m-1)PV_0\,. \qquad (14)$$

Here U_* is the particle velocity in the powder, U is the particle velocity in the monolithic body, and $m = V_{00}/V_0$, where V_{00} is the powder volume and V_0 is the monolithic body volume.

From the U_* value found from Eqn (14) at constant pressure and powder density one can determine the corresponding shock-wave velocity D_*. In a particular range of pressures the calculated U_* and D_* values can be described by an equation similar to Eqn (4)

$$D_* = a + bU_*\,.$$

The results of calculations using this equation are in agreement with the experimental data for powders with moderate porosities. But as the sample porosity increases, the parameters a in the experimental Hugoniot equations decrease down to zero. Unlike c_0, the parameter a cannot be treated as the bulk sound velocity in the porous material; its value lies in the range between the sound velocity inside the grain and the speed of slow motion of the grains involved in 'relay'-type sound transmission in the sample. This approach corresponds to the Touvenin model,[36] which considers powders as systems of plates that transmit perturbation in a porous medium.

It was experimentally shown that the behaviour of a powder under shock compression differs from that of a monolithic body. For instance, experiments involving throw of aluminium and copper impactors in porous aluminium ($\rho = 63\%$ of the density of monolithic body) showed that the same pressure corresponds to different shock-wave velocities (difference is 300 m s^{-1}) while different pressures are measured at the same shock-wave velocities in the powder, depending on the impactor material.[37] This effect is impossible under shock compression of monolithic bodies.

The Hugoniot parameters

$$D_{1,2} = c_{1,2} + \lambda_{1,2}\,U_{1,2} \qquad (15)$$

of a binary mixture (alloy) composed of the solids 1 and 2 can be calculated using the additivity scheme

$$U_{1,2}^2 = xU_1^2 + (1-x)U_2^2\,, \qquad (16)$$

where x is the mass fraction of a component. Relation (16) has the sense of the law of energy conservation, because the energy of a mass unit of the mixture equals the sum of the energies of the components that experienced shock compression at the same pressure.

If the Hugoniot adiabats of components are unknown, one can use their mechanical characteristics and sum the B/ρ ratios of the components 1 and 2 with allowance for their mass fractions (because these parameters have the dimension of energy) and then determine the coefficients $c_{1,2}$ as follows

$$c_{1,2} = \sqrt{\frac{B_1}{\rho_1}x + \frac{B_2}{\rho_2}(1-x)}\,,$$

where $\lambda_{1,2}$ is the weight-average value of λ_1 and λ_2 owing to a small difference between these parameters.

The dynamic pressure produced by shock waves differs from static pressure by very short duration of the periods of pressure rise ($\sim 10^{-12}$ s) and stationary action ($\sim 10^{-6}$ s). Tensile stress (negative pressures) produced in the solid in the unloading wave allows the shock wave to reach the surface of the sample, which is accompanied by spalling phenomena. These features can cause basically new effects under the action of shock waves on substances compared to those observed at high static pressures.

Whereas determination of dynamic pressures presents no severe difficulties, measuring the shock temperatures is a rather complicated task. In this case the most objective thermocouple method is slow, while optical pyrometry data (this technique is characterised by very short time delay) are interpreted under assumptions (blackbody model, uniform emission of radiation from the surface) that require experimental check-up. A recently proposed, new promising technique for measuring the shock temperatures involves the use of NMR spectroscopy. To date, it was only employed in a study of molybdenum.[38] Experimental shock Hugoniots of heated substances are necessary for solving a number of physicochemical problems. However, their number is limited. Such adiabats can be obtained by measuring the bulk elastic moduli at different temperatures.

There is a few crystals with known shock compression characteristics at different temperatures. These are NaCl and LiF,[18] Mo[5] and SiO_2.[39] Heating of the first two materials from 25 to 400 °C causes a decrease in c_0 from 3.3 to 2.9 km s^{-1} (NaCl) and from 5.0 to 4.5 km s^{-1} (LiF); the parameter λ decreases from 1.7 to 1.5 (NaCl) and from 1.5 to 1.3 (LiF). The same parameters of molybdenum vary in different fashion on heating from room temperature to 1400 °C; namely, c_0 changes from 5.14 to 4.78 km s^{-1} while λ changes from 1.22 to 1.42. In glassy SiO_2, the bulk sound velocity (~ 0.75 of the longitudinal sound velocity) increases from 4.46 to 4.84 km s^{-1} in the temperature range 20–1050 °C. In molten SiO_2, it increases from 4.90 to 4.93 km s^{-1} in the temperature interval from 1530 to 2010 °C.

The bulk elastic modulus of ZrO_2 and its pressure derivative (265 GPa and 4.0, respectively) remain unchanged in the temperature range from 25 to 1400 °C,[40] but since the density of the body decreases on heating in this case, it follows from Eqns (10) that the coefficient c_0 increases while the parameter λ retains its value. The results of B_0 measurements for a number of metals at −273 (B_1) and 27 °C (B_2) showed [41] a decrease in this parameter on heating.

Element	Al	Cu	Fe	Pb	α-Pu
B_1/B_2	1.075	1.036	1.030	1.104	1.303

A large change in the elastic modulus of α-Pu is due to changes in the 5f-electron shell of plutonium atom.

No general trend in the influence of temperature on the parameters of Eqn (4) has been revealed so far. This effect should be studied in each particular case.

2. Recovery of shock compression products

Ryabinin [42] pioneered in the recovery and investigation of the products of shock compression of chemical compounds. Despite the lack of interesting chemical results, his study opened a new research avenue in the physics of shock waves, which was called

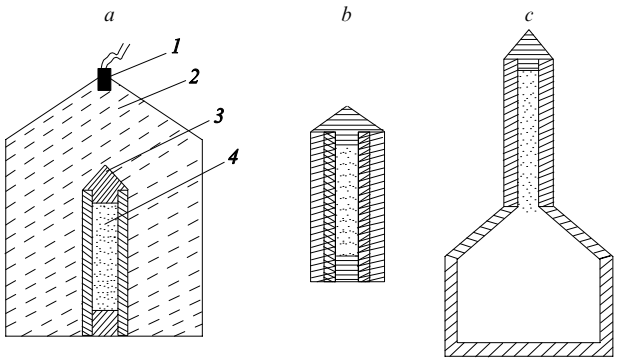


Figure 3. Schemes of experimental setups with cylindrical recovery ampoule (*a*), cylindrical recovery ampoule with layered shell (*b*) and recovery ampoule with large cavity (*c*).
Detonator (*1*), explosive (*2*), ampoule (*3*) and sample to be compressed (*4*).

'recovery experiments'. Later on, cylindrical ampoules employed by Ryabinin were significantly simplified and modified. Here we will consider the main types of such ampoules.

Figure 3 *a* presents a scheme of typical experimental setup with a steel cylindrical ampoule. The modification of the ampoules consists in the use of layered shells made of different materials (Fig. 3 *b*). The shells provide a stepwise loading of the substance by shock waves owing to difference between the shock-wave velocities in different materials. Yet another modification consists in the use of an attached large container (Fig. 3 *c*) for expansion (scattering) and subsequent quenching of shock compression products in the course of unloading. Prior to explosion, the cylindrical ampoules can be heated [43] or cooled (by, *e.g.*, liquid nitrogen) in order to adjust the thermodynamic conditions. To the same end, water or other substances with high heat capacity can be added to the sample to be compressed (they absorb heat and thus provide corresponding cooling).

In the case of uniformly distributed charge of the explosive, cylindrical ampoules provide an axially symmetrical compression of the substance with minimum deformation of the sample. However, if the explosive is concentrated within some sectors of the cross section (Fig. 4), a strong deformation of the ampoules can be achieved. If the empty regions in the charge (see positions *1* in Fig. 4) are filled with materials of different mechanical hardness, it is possible to control the degree of the ampoule deformation.

Owing to very high pressure in the axial (Mach) region, cylindrical ampoules are, as a rule, used for the synthesis and modification of chemical compounds. If the thermodynamic parameters in this region are to be reduced, cylindrical ampoules with a metallic rod at the centre are employed. This allows repeated reflection of the shock wave from the rod and walls, thus causing the pressure to increase with minimum heating of the substance.

An important modification was the invention of dynamic–static compression ampoules [44] where the compound is surrounded by the working substance (*e.g.*, KBr) which undergoes a reversible phase transition. Under loading, KBr undergoes a structural transition of the NaCl → CsCl type accompanied by a 15% reduction of the volume, while in the unloading stage potassium bromide should return to its initial state. However, the hard recovery ampoule, which is made of strain-hardening steel and therefore becomes even harder during shock compression, makes the expansion of the working substance impossible. As a result, a residual (static) pressure is produced inside it (Fig. 5). The internal static pressure equal to the phase transition pressure (2 GPa) is rather high; this precludes annealing of thermally unstable high-pressure phases, in particular, a Würtzite-type boron nitride (w-BN) polymorph.[45]

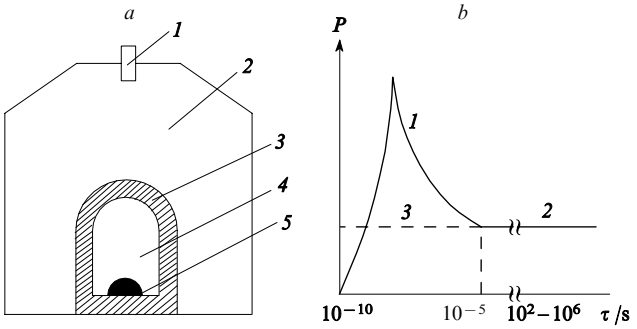


Figure 5. Experimental setup for dynamic-static compression (*a*) and corresponding pressure–time diagram (*b*).
(*a*) Detonator (*1*), explosive (*2*), ampoule (*3*), working substance (*e.g.*, KBr) (*4*) and sample to be compressed, *e.g.*, graphite-like boron nitride (g-BN) (*5*).
(*b*) Temporal evolution of dynamic pressure (*1*), static pressure (*2*) and phase transition pressure (2 GPa for KBr) (*3*).

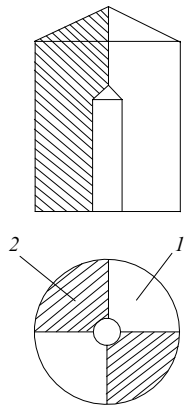


Figure 4. Sections of cylindrical ampoule with sector arrangement of explosive.
(*1*) Air (or other inert material), (*2*) explosive.

Another group of recovery systems includes plane ampoules in which pressure is produced using a mud cap (Fig. 6 *a*) or by throw of impactor plate (Fig. 6 *b*). By varying the composition of the explosive, the material and the thickness of the impactor plate it is possible to change the magnitude and duration of the dynamic pressure. Additionally, such systems provide a better possibility

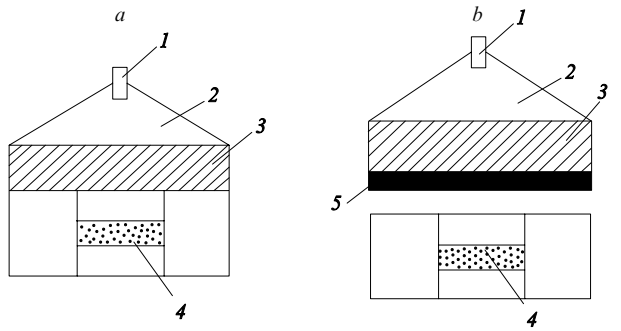


Figure 6. Schemes of plane recovery ampoules employed under shock compression using a mud cap (*a*) and throw of an impactor (*b*).
Detonator (*1*), plane wave generator (*2*), explosive (*3*), sample to be compressed (*4*) and impactor plate (*5*).

for heating of the substance under study without contact between the ampoule and explosive before explosion. Uniaxial loading in plane ampoules is convenient for pressure measurements and calculations, but the design of the experimental setup is labour-consuming. Plane ampoules are most often used for explosive compaction or pre-activation of brittle powders, because in this case the thermodynamic parameters in the bulk of the sample are the same and can easily be controlled. Forced high-strain-rate deformation of samples also appeared to be efficient for compaction. To this end, the diameter of the pellet made of the substance under study should be smaller than the diameter of the ampoule. Planar impact is followed by plastic flow of the sample across the inner section of the ampoule, which sometimes results in transparent samples of rather strong materials.

Stepwise loading of samples in plane ampoules is attained using layered shells or impactors. Here, the temperature of the substance compressed is much lower (isentropic compression) than in the case of single-shot loading with the same explosive. In order to increase the pressure in the plane recovery ampoules, schemes with counter-propagating shock waves are used (Fig. 7). Other types of plane recovery ampoules were described in a review [46] and in a monograph.[4]

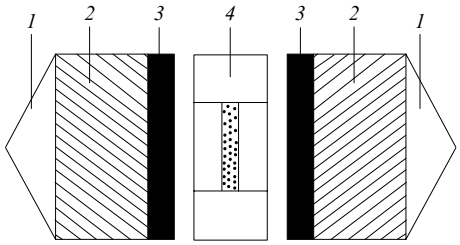


Figure 7. Scheme of a device for shock compression experiments using counter-propagating shock waves.
Plane wave generator (*1*), explosive (*2*), impactor (*3*) and sample to be compressed (*4*).

The most industrially important procedure for recovery of explosion products involves placing a mixture of the substance under study and the explosive in a mechanically hard chamber for preservation of the expanding detonation products. For better annealing of detonation products, the charge is surrounded by an ice shell. The advantage of this technique consists in the absence of recovery ampoules, which makes the process much cheaper. Additionally, expansion of products within a large cavity causes annealing of high-pressure phases. The detonation parameters of, *e.g.*, TNT ($P = 18.4$ GPa, $T = 2900$ °C) are sufficient to ensure transformation of graphite to diamond. As a result, the yield of diamond upon detonation of a graphite–explosive mixture or a pure explosive giving carbon as a solid detonation product can be as high as tens per cent. This is an order of magnitude higher than the yield provided by the ampoule technique (although the detonation diamond particles are much smaller than the particles obtained using the ampoule method). In Russian Federation, detonation diamonds are produced on a large-scale basis.

Probabilistically (assuming a homogeneous detonation cloud), the formation of detonation diamonds in the form of clusters comprising about $\sim 10^4$ atoms is impossible. Indeed, detonation of TNT or TNT–RDX alloys gives H_2, CO, CO_2, H_2O, NO, NO_2, carbon clusters C_n ($n = 1-6$), *etc.* as products. Even if we restrict ourselves to these products, the probability of formation of a diatomic carbon cluster in the detonation cloud equals 1/7, the addition of the third and fourth carbon atom reduces the probability to 1/49 and 1/343, respectively, *etc.* Therefore, the probability of formation of a cluster comprising ten carbon atoms approaches zero. Nevertheless, the number of atoms in the actually formed clusters is three orders of magnitude larger!

We believe that this can be explained by heterogeneous (layered) structure of the detonation cloud. The layers mainly include carbon atoms or hydrogen or water molecules, *etc.* The formation of layers can be understood if we assume that, upon detonation, all fragments of the explosive molecule have the same kinetic energy of $mv^2/2$ (m and v are the mass and velocity of a molecular fragment). Then, the velocities of the detonation products are inversely proportional to $\sqrt{m}$ and the detonation cloud will contain layers of atoms or molecules of different masses. Formation of diamond clusters will occur in the layer that comprises mainly carbon atoms. Similar masses of different molecules in the same layer impose a limitation on the growth of cluster and it is contaminated with impurities, which is observed in the experiments.

Methods of preservation of the shock compression and detonation products are used for chemical purposes, namely, for performing phase transformations and synthesis of novel compounds. Shock-induced syntheses and compaction, pre-sintering and catalytic activation of brittle materials have been documented in a review.[47]

III. Features of phase transitions in shock waves

Iron shock compressibility studies [48] revealed a break in the Hugoniot curve at 13 GPa, corresponding to the α-Fe → ε-Fe transition. Analysis of ε-Fe fragments found upon disruption of target unambiguously indicated a phase transition with a duration of $\tau \leqslant 10^{-6}$ s. Optical studies [49, 50] showed that transitions under shock compression occur 10^7-10^{14} times faster than in static experiments.

What is the reason for high rate of the phase transitions under dynamic compression?

Variation of the bond lengths in crystals upon polymorphic transformations lie within the range of amplitudes of thermal atomic vibrations ($\sim 10\%$ of the bond length). Therefore, the duration of the phase transition can be estimated from shock-induced thermal atomic jumps. The action of shock waves causes fragmentation of crystalline grains, produces vacancies and dislocations in them and also causes heating of the body to very high temperatures, which favours intensification of atomic vibrations. The frequency of thermal vibrations is given by

$$w = A\sqrt{\frac{kT}{m}}, \tag{17}$$

where A is a constant, k is the Boltzmann constant and m is the atomic mass. At room temperature, for hydrogen atom one has $w = 6 \times 10^{13}$ s^{-1} and $\tau \approx 2 \times 10^{-14}$ s; for $m = 100$ the time changes by an order of magnitude; with allowance for high pressure and activation energies [51] one gets $\tau \approx 10^{-12}$ s, which is in agreement with experimental data.

Intensive studies of polymorphic transformations of simple bodies (elements) and compounds under shock compression began in the mid-1950s. Experiments showed that the dynamic phase transition pressures are similar, often being somewhat higher than the static transition pressures. This is due to the hydrostatic character of shock compression (see above) and to the fact that the dynamic loading temperature is higher than the temperature at which static experiments are carried out (usually, room temperature).

Analysis of the available experimental data made it possible to solve a number of fundamental problems concerning the kinetics and mechanisms of shock-induced phase transitions. We will consider these problems from the structural point of view, based on the experimental data only.

First of all, mention should be made of the anisotropy of phase transitions in the crystals of alkali metal halides. Namely, if the crystallographic axis ⟨111⟩ is normal to the shock wave front, the NaCl → CsCl type transitions occur at lower pressures, which

corresponds to compression of the unit cell along its spatial diagonal.[52] This mechanism was studied in more detail using KCl samples; the phase transition points at 2.5, 2.2 and 2.1 GPa along the ⟨100⟩, ⟨110⟩ and ⟨111⟩ directions, respectively, were observed.[53] The anisotropic phase transition was explained in terms of atomic displacements along the spatial diagonal of the unit cell. However, coherent atomic displacements cannot cause transformation of the graphite lattice into the diamond lattice. Phase transitions require destruction (amorphisation) of the starting crystalline graphite. This conclusion is substantiated by the maximum yield of diamond in the detonation-induced transformation of the most defect carbonaceous material, namely, carbon black.

Analysis of these experimental findings gave an impetus to studies on geometric modelling of phase transitions that served as a basis for a separate avenue of scientific research.[54]

In the graphite–hexagonal diamond (lonsdeilite) and g-BN–w-BN systems both the initial and final modifications have the same symmetry and the phase transition is driven by the puckering of planar hexagonal graphite sheets accompanied by the formation of sp^3-bonds between the close-lying atoms belonging to neighbouring sheets. A metastable g-BN phase was detected[55] with an interplanar separation of 3.28 Å, which is smaller than in the single crystal (3.33 Å), and 002 X-ray reflections are broadened owing to structural deformation in this direction. Annealing of the würtzite-type BN polymorph causes the formation of the g-BN phase by the same mechanism, but in the reverse order.[56]

Shock compression of CdF_2, CaF_2 and CuBr results in reduction of the unit cell parameters by 0.002, 0.003 and 0.047 Å, respectively (lattice parameters were measured with an accuracy of ±0.0005 Å) with retention of the unit cell symmetry and valences of the metal atoms.[4] Isomorphic reduction of unit cell parameters after shock compression was small, but the dielectric constants (ε) responsible for the character of chemical bonding changed substantially, namely, they increased from 7.1 to 7.9 for fluorite and from 10.0 to 17.8 for CuBr. This is quite clear, since even a small shortening of the distance compared to the equilibrium value causes a dramatic strengthening of electron interaction and an increase in the atomic polarisabilities. Heating of isomorphically compressed crystals is accompanied by exothermic effect and the crystal structures and properties return to the initial state.

Isomorphic transitions also occur under the action of high static pressures. For instance, the unit cell parameters of samarium chalcogenides are dramatically reduced owing to an increase in the valence of the metal [Sm(II) → Sm(III)]. In dynamic experiments isomorphic reduction of structural parameters is due to quenching of the shocked samples that occurs with retention of the oxidation state of the atoms.

Specific phase transitions were detected under shock compression of Nb_2O_5 and Ta_2O_5 crystals. Shock compression causes minor changes in the composition and results in the formation of TiO_2-type structures.[57] Therefore, this transition is followed by the formation of a structure in which 20% of sites in the metal lattice are vacant (*i.e.*, compounds of the $M_{0.8}O_2$ type are formed). Shock compression of Ln_2S_3 (Ln = Tb, Dy, Ho, Er, Y) causes a $Ho_2S_3 \rightarrow Th_3P_4$-type structural transition; here, each ninth site in the metal sublattice is replaced by a vacancy.[58] A similar transformation was observed under shock compression of CeF_4, ThF_4 and UF_4. These fluorides experienced a $ZrF_4 \rightarrow LaF_3$ structural transition accompanied by the formation of 25% vacant sites in the cation sublattice (*i.e.*, $MF_4 \rightarrow M_{0.75}F_3$ transition).[59] Such transformations were not detected under static compression, because denser structures with ordered system of defects are retained only upon rapid quenching of corresponding phases during the shock-wave unloading.

An interesting phase transition occurred in TiO under shock. The initial phase belongs to the monoclinic system (a = 5.85, b = 9.34, c = 4.14 Å, β = 107°32′). After shock compression the diffraction pattern exhibited no weak lines while the intense lines corresponded to cubic latice with a = 4.176 Å. In this case the phase transition accompanied by an increase in symmetry is also driven by generation of numerous defects that are characteristic of this crystal.[60]

As shown above, the shock wave technique makes it possible to produce negative pressures that can be realised in the rarefaction wave in the form of tensile stress in the samples under study. Phase transformations at negative pressures can result in the formation of loose structures that cannot appear at $P \geqslant 0$. Such a structure was first found in our study of turbostratic BN under shock compression. We found a very small amount of a new polymorph (E-phase)[61] whose density was lower than that of w-BN. The last-mentioned phase is formed only after annealing of defects and corresponding increase in the degree of crystallinity of the initial graphite-type boron nitride polymorph (w-BN is formed under shock compression of g-BN if the density of the starting phase is at least $\geqslant$2.2 g cm^{-3}). The Hugoniot adiabats of the BN samples with different densities show a similar trend.[4] The structural parameters of E-BN are very similar to those of a certain fullerene phase:[62, 63]

Parameter	a /Å	b /Å	c /Å	ρ /g cm^{-3}
E-BN	11.14	8.06	7.40	2.50
C_{60}	11.16	8.17	7.58	2.50

It is important that the E-phase is formed under shock compression only in the axial region of cylindrical ampoules if there is a cavity that appeared under the action of tensile stress in the compressed material after irregular collisions of shock waves. More recently, this phase was obtained by researchers from other groups under the action of various physical factors on g-BN.[64–69]

Now we will consider yet another unusual type of phase transitions, which is atypical of physics of high static pressures. Usually, heating is accompanied by polymorphic transformations with the formation of looser structures, but there exist a number of crystalline compounds (*e.g.*, PbO, MnS, Ln_2S_3, Ln_2O_3, TiO_2, ZrO_2 and LnF_3) that undergo phase transitions accompanied by densification upon heating. Under shock compression these compounds are transformed into phases with lower density (compared to the initial phase) and looser atomic structure (Table 6).

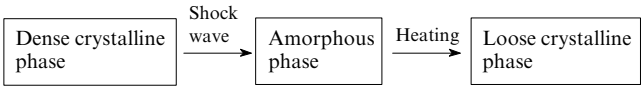
Table 6. Characteristics of anomalous phase transitions.[70]

Composition	Initial phase		After shock compression	
	structural type	ρ /g cm^{-3}	structural type	ρ /g cm^{-3}
Tm_2S_3	Ho_2S_3	6.27	new type	6.06
Nd_2O_3	A-form	7.42	C-form	6.29
SmF_3	LaF_3	6.93	YF_3	6.64
HoF_3	LaF_3	7.83	YF_3	7.64
GeSSe	α-phase	4.0	γ-phase	3.6
GeSTe	α-phase	5.1	γ-phase	4.7
GeSeTe	α-phase	5.6	γ-phase	5.2
ZrO_2	tetragonal	6.03	monoclinic	5.83
PbO	orthorhombic	9.72	tetragonal	9.43

Anomalous phase transitions accompanied by loosening upon dynamic compression were explained by the action of negative pressures, however detailed studies revealed a more complex phenomenon. Under the action of a shock wave the lattice of the solid is disordered, dislocations are produced, and at higher concentration of defects the crystalline compound transforms to amorphous substance with minimum density (for the given composition). Heating of such a material causes its crystallisation in a phase with minimum density. Upon further heating the material crystallises in a denser phase. This mechanism was experimentally proved taking GeSeTe[71] and Nd_2O_3[72] as exam-

ples. Here, amorphous phases transformed into crystalline modifications with minimum density upon heating. The temperatures of successive transitions can differ insignificantly; besides, it is difficult to reach the desired range of thermodynamic parameters under shock compression. Therefore, these transitions have not long been detected.

Thus, an anomalous phase transition can be described by the following scheme:



Correctness of this scheme is substantiated by occurrence of anomalous transitions under static shear compression and upon intense irradiation.[4]

The structural approach to the description of the features and mechanisms of phase transitions under shock compression (see above) is not unique. For instance, the kinetic and thermodynamic aspects of this problem were also considered.[73]

IV. Duration of solid-phase chemical reactions

1. Measurements of the duration of solid-phase reactions

The fact that the shock compression time is sufficient for a phase transition to occur was experimentally established in 1956.[48] As to solid-phase reactions, this was a moot question for long, because either synthesis or decomposition of chemical compounds in the recovery ampoules can occur both under shock and after unloading due to residual heat.

A solid-phase reaction proceeds in several steps. These are fragmentation of grains and cleavage of chemical bonds in the initial components, mixing of different reagents to bring them into contact at the atomic level and, finally, growth of new-phase crystals to a size that ensures their existence. Since diffusion in solids is slow, being even slower at high pressures (its rate is at least six orders of magnitude slower than the rate required for the synthesis on the microsecond time scale), solid-phase reactions seemed to be hardly probable. At the same time, gas–solid and liquid–solid chemical interactions that take a few microseconds have long been known (see, *e.g.*, Refs 74 and 75).

Actual duration of solid-phase reactions under shock compression was determined by measuring the time of the onset of heat release in exothermic reactions, by search for high-pressure phases among the synthesis products, by elucidating mechanical after-effects of shock-induced transformations in the recovery ampoules and, finally, by measuring the shock-wave velocities and pressure in the reacting mixtures.

a. Temperature measurements

Thermocouple measurements of the temperature of the reaction

$$Sn + S \longrightarrow SnS$$

were carried out in our research group since 1968 for a period of two decades. The duration of the experiments gradually shortened from 10^{-1} to $\leqslant 10^{-4}$ s due to the use of thinner thermocouples and improvement of experimental procedure (see references cited in Ref. 76). Measurements were carried out in the recovery ampoules rigidly joined to massive metallic slab in order to ensure immobilisation of the ampoules during the explosion. In order to obtain objective information, the dynamic compression was carried out under the same conditions for the reacting mixture Sn + S, individual components (Sn, S) and reaction product (SnS). Experiments showed that the residual temperatures of these individual compounds measured 0.1 s after explosion varied in the order $110 \rightarrow 120 \rightarrow 130$ °C, whereas that of the reacting mixture reached a value of 1110 °C, which corresponds to a 50% chemical conversion.

The results of X-ray diffraction study of the samples of the recovered products taken from different regions of the ampoule showed that the synthesis occurs mainly in the axial region of the cylinder (in the so-called Mach stem) and the extent of conversion and the product composition (SnS or SnS_2) depend on the dispersion of the initial powder, which indicates a solid-phase character of the reaction.

The results of thermocouple measurements were checked calorimetrically. After an accurately measured time interval (from several tens of seconds to 1–2 min) after explosion, the recovery ampoule containing the reacting mixture and the product was taken out of the explosion chamber and placed in a water calorimeter. After cessation of heat release in the calorimeter, the temperature of the ampoule was calculated. Then, the ampoule was taken out of the calorimeter, heated in a furnace to a certain higher temperature and again placed in the explosion chamber. This was done in order to cool the ampoule under the same conditions as after the explosion. The cooling curve was measured using a thermocouple. Such cooling curves allow an exact extrapolation of the calorimetrically measured temperatures to zero time instant. The results obtained by the two methods differed by a few per cent. In the cylindrical ampoules with the diameter of the orifice in the bottom plug equal to the diameter of the Mach stem, the substance in the axial region was blown away, which made it possible to determine calorimetrically the contribution of the Mach region to the overall enthalpy of the sample.

Further shortening of the duration of the temperature measurements in the reacting systems was attained by using an optical pyrometer. The results of the studies of $Al + Fe_2O_3$,[77] Ni + Al,[78,79] Sn + S,[80] and Sn + Te mixtures[81] showed that the synthesis is completed after nearly 10^{-7} s. It is significant that for the Sn + S mixture the dependence of the temperature changes on the pressure applied passes through a maximum (Fig. 8). This indicates that the reaction can occur in a limited range of pressures. Raising the pressure favours SnS formation, which is accompanied by compaction, but simultaneously the thermal effect (and, hence, the thermodynamic driving force) of the reaction decreases.[76]

Real-time studies of the temperature dependences of the shock-induced interaction of magnesium, aluminium and titanium with sulfur were reported.[82–84] The reaction durations were about 50 ns and the extent of conversion varied from 0.2 to 0.5. An optical study of the Al–S system revealed a dependence of the rate of the shock-induced reaction on the dispersity of the reacting particles, which proves the solid-phase character of the process. Under explosive loading using a TNT–RDX alloy the Mg–S system shows that the first temperature rise region is followed by a region of gradual increase in temperature due to the development of the reaction after unloading. This can serve as a model for the situation in the recovery ampoules.

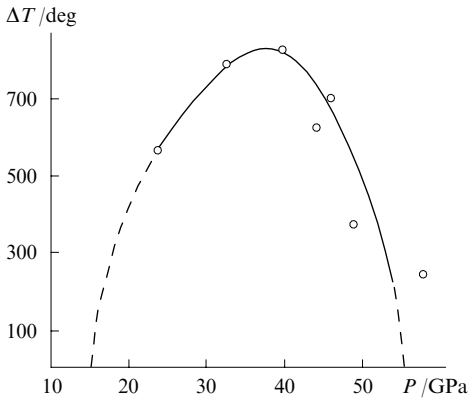


Figure 8. Shock temperature plotted *vs.* pressure in Sn + S reacting mixture.

b. Kinematic measurements

Kinematic measurements (*i.e.*, measurements of parameters under shock compression) provide objective information on possible chemical transformations in a mixture of solids. Deviation of the shock compression curve of Sn + S mixture [85] toward a larger volume and/or pressure at $P \geqslant 15$ GPa was the first direct proof of the fact that the duration of a solid-phase reaction is of the order of a few microseconds. More recently, chemical reactions in shock waves were detected in the compressibility studies of Sn + Te (at $P > 45$ GPa),[81] Ti + C (at $P > 15$ GPa) [86] and Ti + Ni (at 3.2 GPa) mixtures.[87] According to unpublished data obtained by G A Adadurov and S V Pershin (N N Semenov Institute of Chemical Physics, Russian Academy of Sciences), the shock compressibility curves of Fe + S and Cu + Al mixtures exhibit kinks at 28 and 32 GPa, respectively, upon increase in volume (Fig. 9).

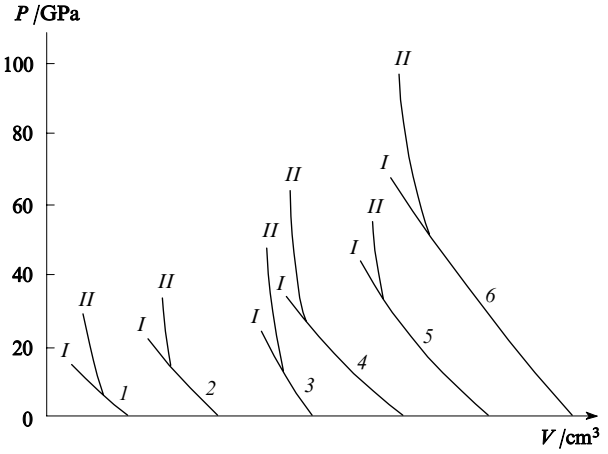


Figure 9. Kinks in the shock compressibility curves of various smixtures in the region of chemical interaction.
Ni + Ti (~7 GPa) (*1*), Sn + S (~15 GPa) (*2*), Ti + C (~15 GPa) (*3*), Fe + S (~28 GPa) (*4*), Cu + Al (~32 GPa) (*5*) and Sn + Te (~55 GPa) (*6*); in all cases *I* refers to the mixture and *II* refers to the product.

Generally, the chemical interaction between the components of a mixture can be accompanied by either a decrease or an increase in volume. For the compositions M^zX^{8-z} (X = Cl, Br, I; S, Se, Te; P, As, Sb), the synthesis of compounds of Group 1B, 2B and 3B metals leads to an increase in the volume, whereas the synthesis of compounds of Group 1A, 2A and 3A metals leads to a decrease in the volume (this is partially compensated by an increase in the volume due to thermal expansion). The magnitude of the changes in the volume can be estimated with ease. Indeed, the exothermic effect lies in the range 100–200 kJ mol^{-1}, the heat capacity is of the order of 40–50 J (mol K)$^{-1}$ and the temperature of the substance increases to 2000–4000 °C. The thermal expansion coefficients of solids are about 2×10^{-5}; therefore, these temperature changes cause the volume to increase by 4%–8%. Physical measurements showed that the degree of conversion in shock waves is at most 0.5; therefore, the actual increase in volume due to thermal expansion is 2%–4%. It is these numerical values that should be used when comparing the volumetric changes occurring as a result of a chemical reaction.

As typical examples, we will consider changes in the molar volumes of the low-pressure phases in the reactions

$$M + S \longrightarrow MS,$$

where M = Zn, Ca.

Calculations were performed using the expression

$$V = V_0\left(1 - \frac{U}{D}\right), \tag{18}$$

derived by combining Eqn (1) and Eqn (2). Here V and V_0 are the initial and final volumes of the body, D and U are the shock and particle velocities (see Section II). For ZnS, the U and D values can be determined from the experimental Hugoniot adiabat [88] and for CaS this can be done using the Hugoniot adiabat reconstructed from Eqns (10) and the results of supersonic measurements of B_0 (64 GPa) and B_0' (4.2). For Zn + S and Ca + S mixtures, the particle velocities can be calculated using the additivity scheme from the Hugoniot adiabats of the elements (see Table 2) and Eqn (16). Having determined the $U_{1,2}$ values for a number of the pressure values and knowing the density of the mixtures, one can calculate D_1 using expression (15) and then the V values from Eqn (18). The $P = f(V)$ dependences were established using the following characteristics:

for Zn + S

$D = 2.085 + 1.804\,U$, $\rho = 3.95$ g cm^{-3};

for ZnS

$D = 3.13 + 1.30\,U$, $\rho = 4.085$ g cm^{-3};

for Ca + S

$D = 2.93 + 1.13\,U$, $\rho = 1.73$ g cm^{-3};

and for CaS

$D = 4.95 + 1.30$ U, $\rho = 2.61$ g cm^{-3}.

Since the synthesis of zinc and calcium sulfides is accompanied by heat release (Q), one should take into account the additional 'thermal pressure' ΔP_Q. According to the Mie–Grüneisen model, at $\Gamma V = \text{const}$ it can be calculated using an approximate relation

$$\Delta P_Q = \frac{2\Gamma Q}{V(\Gamma + 2) - \Gamma V_0}. \tag{19}$$

The Q values for ZnS and CaS are 191.8 and 473.2 kJ mol^{-1}, respectively (see Ref. 89). In fact, the conversions in shock waves are at most 50%; therefore, the parameters of Eqn (19) are as follows: 0.5 Q, $\Gamma = 0.68$ (ZnS) [88] and $\Gamma = 1.41$ (CaS).[90]

Finally, we must allow for the change in the thermal effect due to the different compressibility of the mixture and the product. The difference in the shock compression work

$$E_c = \frac{P(V_0 - V)}{2}$$

between the mixture and the product in the M + S → MS system causes a decrease in Q by

$$\Delta E_c = E_c(M + S) - E_c(MS).$$

Table 7 presents the results of the $V = f(P)$ calculations using the relations listed above and the P^* values for the heated compounds obtained by summation of the P and ΔP_Q values. Analysis of the data in Table 7 and the plots in Fig. 10 shows that the $P-V$ Hugoniot curve deviates towards larger volumes upon the formation of ZnS and towards smaller volumes for the synthesis of CaS. Raising the pressure causes the curves for CaS and Ca + S to approach each other.

This result is important for the understanding of the processes occurring, *e.g.*, under shock compression of a Mo + 2 Si mixture. A kink in the $P-V$ plot towards smaller volumes in the pressure range 6.5–7 GPa was interpreted [91] as a result of the melting of silicon and corresponding increase in the compressibility of the mixture. It was assumed [91] that capillary flow of molten silicon limits the deformation of the molybdenum particles and mixing between the reactants. However, in another study by these authors a partial interaction in the same system, detected in the recovery experiments was interpreted as a reaction of solid molybdenum with molten silicon.[92] According to Vreeland,[93] the reactions of titanium, niobium and molybdenum with silicon proceed by

Table 7. Changes in molar volumes during shock-induced syntheses M + S ⟶ MS.

P /GPa	V (see [a])	E_c (see [b])	V (see [a])	E_c (see [b])	Q (see [b])	ΔP_Q /GPa	P^* /GPa
Mixture Zn + S			Compound ZnS				
0	24.68	0	23.86	0	95.9	0	0
3	21.98	4.05	22.35	2.25	94.1	2.93	5.93
6	20.62	12.2	21.23	7.9	91.6	3.06	9.06
9	19.71	22.35	20.35	15.8	89.35	3.17	12.17
12	19.03	33.9	19.62	25.45	87.45	3.27	15.27
15	18.50	46.35	19.01	36.4	85.95	3.37	18.37
Mixture Ca + S			Compound CaS				
0	41.70	0	26.74	0	236.6	0	0
5	33.32	20.95	24.99	4.37	220	13.0	18.0
10	29.31	61.95	23.70	15.2	189.8	12.4	22.4
15	26.77	112.0	22.69	30.4	155.0	11.0	26.0
20	24.95	167.5	21.87	48.7	117.8	9.0	29.0
25	23.56	226.7	21.18	69.5	79.4	6.5	31.5

[a] In $cm^3\ mol^{-1}$; [b] in $kJ\ mol^{-1}$.

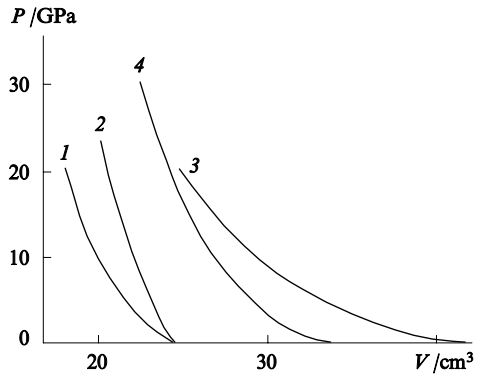


Figure 10. Shock compressibility curves for various mixtures. Zn + S (*1*), ZnS (*2*), Ca + S (*3*) and CaS (*4*).

heterogeneous (liquid – solid) mechanism. The kink in the $P-V$ curve [91] can be due to the reaction

$$Mo + 2Si = MoSi_2,$$

which is accompanied by a decrease in the volume by 27.7% (see Ref. 94). The heat of the reaction (132 $kJ\ mol^{-1}$) has no effect on the volume ratio, because the volume of the product increases only by a few per cent.

Probably, similar processes also occur under shock compression of Al + SiO_2 mixture. A kink in the Hugoniot adiabat of this mixture with a decrease in the volume was interpreted [95] as a quartz → stishovite transition. The chemical interaction resulting in Al_2O_3 is also accompanied by compaction and release of much higher energy (619 $kJ\ mol^{-1}$ for stoichiometric composition), which makes this reaction preferred. Additionally, the kink in the shock adiabat of the mixture was detected at 20 GPa, whereas the phase transition in pure quartz occurs at 38 GPa. Voskoboinikov [96] analysed the shock adiabats of the mixture and compound and showed that in this case the chemical reaction is more probable than a phase transition.

To decide between the phase transition and shock-induced chemical transformation accompanied by compaction, it is sufficient to measure the temperature, because the heat of a chemical reaction is usually an order of magnitude higher than that of polymorphic transformation. For instance, kinks in the Hugoniot adiabats of CS_2 and C_6H_6 at $P > 6$ GPa with a decrease in volume [97] can be treated as phase transitions. However, the results of optical measurements [98] revealed a stepwise increase in the temperature of the medium by more than 250 °C at these pressures, which indicates a chemical reaction (in this case, decomposition). If the decrease in the volume upon a shock-induced chemical transformation is small, it can be compensated by thermal expansion and the shock adiabat will exhibit no features. For instance, the volumes of organofluorine compounds are changed insignificantly,[99] whereas the changes in the temperature are large, namely, a stepwise increase by 500 °C at $P > 22$ GPa owing to decomposition.[100] Similarly, a shock compression study [101] of teflon at $P > 34$ GPa showed an abrupt increase in the speed of sound behind the shock-wave front and almost smooth shock adiabat curve. A chemical reaction in the Nb + Si mixture substantiated by the recovery experiments was detected from a jumpwise increase in the speed of sound.[102]

Yet another method of detection of physicochemical transformations under dynamic loading is the study of shock wave damping. From general physical considerations it follows that [103]

$$\frac{\partial D}{\partial \tau} = \frac{c}{c + U - D},$$

where c is the speed of sound behind the shock-wave front. A phase transformation accompanied by densification is characterised by an increase in D and a decrease in U; therefore, the damping rate will increase.

Measurements in shock compressed metal – oxide mixtures revealed dramatic changes in the shape of the $P = f(\tau)$ curves after particular pressures were reached.[104] For instance, a fivefold increase in the shock wave damping in the Mg + SiO_2 mixture (sample thickness 2 mm) in the pressure range 24.0 – 28.8 GPa, a twofold increase for the Mg + TiO_2 mixture at 29.6 – 31.2 GPa, a threefold increase for the Mg + Fe_2O_3 mixture at 18.8 – 23.6 GPa and a fourfold increase for the Al + Fe_2O_3 mixture at 17.1 – 22.8 GPa were observed compared to monotonic changes in the damping rates beyond these pressure ranges. In all cases the volumes of products were smaller than those of the starting mixtures. Correspondingly, the deviations of the compressibility curves for these reactions should be opposite in sign compared to the deviations of the compressibility curves for the shock-induced reactions characterised by an increase in volume.

A shock-induced solid-phase reaction

$$Zn + Te \longrightarrow ZnTe$$

was studied using cold and pre-heated mixtures.[105] The shock velocity in the mixture pre-heated to 242 °C showed a jumpwise increase by 0.7 $km\ s^{-1}$. Since an exothermic reaction begins at this temperature, the shock velocity jump can be explained by energy transfer from the chemical reaction to the shock wave in the zone of high dynamic pressure. An increase in the shock velocity induced by exothermic reaction was also revealed in a study of the reaction in the Zn + S mixture.[106]

In 1993, researchers from the USA first reported pressure measurements in the course of chemical transformations using piezoelectric transducers; in particular, a reaction with a microsecond duration was detected in the Ti – Si system. A review of corresponding studies is available.[107]

c. Estmation of the reaction duration from mechanical changes in recovery ampoules

The temperature and kinematic measurements are labour-consuming and therefore cannot be used for quick analysis of the duration of chemical transformations under shock compression. Taking into account the fact that shock-induced synthesis occurs mainly in the axial region of cylindrical ampoules (Mach stem whose size is determined by the energy supplied), the reaction can be detected from the change in the Mach stem diameter and from the action of the Mach stem on the bottom of the ampoule (spall plate) behind the shock wave front.[108]

Shock compression experiments carried out under the same conditions revealed a larger diameter and deeper spall for the Sn + S mixture compared to SnS, the mass of the spall plate being 0.06 and 0.003 g, respectively. Since the velocity of the motion of the spall element is given by

$$v = 2U,$$

for this system one gets $v = 4.3$ km s^{-1}. From here the kinetic energy of the spall plate, E is about 60 kJ mol^{-1} for the mixture and nearly 3.2 kJ mol^{-1} for the compound. The difference, ~ 57 kJ mol^{-1}, is the increase in energy equal to the contribution of the heat of the chemical reaction to the energy of the Mach wave. This difference corresponds to an extent of conversion of 30%, which is similar to the reaction yield determined from the temperature and kinematic measurements.

Similar spalling features in the Sn + Te system were observed using more energetic explosives ($D_0 = 7.3$ km s^{-1}) and, correspondingly, at a higher pressure of the onset of the chemical reaction detected in kinematic measurements.

Studies of spalling phenomena in the recovery ampoules during shock compression of Ti + C and Zn + S mixtures using explosives with a detonation velocity of 6.2 km s^{-1} in the former and 7.2 km s^{-1} in the latter case showed the formation of compounds TiC and ZnS in ~ 7 and ~ 90% yields, respectively.[109] A regular decrease in the Mach stem diameter with an increase in the stiffness difference (ρc^2) between the shell and the content of the cylindrical ampoule was also established in that study. The stiffnesses of compounds TiC and ZnS are higher than those of the corresponding mixtures; therefore, a decrease in the difference in ρc^2 between the shell and the substance under study causes extension of the Mach region in the shock compressed material.

Endothermic transformations lead to narrowing of the Mach stem. A dark Mach stem appeared in the axial region of the cylindrical ampoule at a distance of about two diameters from the upper end upon shock compression of CuCl. The downward motion of the Mach stem was accompanied by its monotonous extension in a conical fashion. Once a certain intensity was reached, the substance in the Mach zone melted and the Mach stem narrowed; further motion toward the bottom of the ampoule was again accompanied by extension of the Mach stem until the next melting of the powder.

2. Solid-phase reactions

The formation of high-pressure phases as a result of a chemical reaction indicates that the reaction proceeds in the high-pressure zone. To date, a large body of experimental data on the decomposition and synthesis reactions has been accumulated. In the former case the interacting atoms are inside molecules or coordination polyhedra of crystals, *i.e.*, they can be treated as being in contact with one another, the decomposition occurs instantaneously and time is only taken for the separation and nucleation of a new phase. The latter case requires dispersion and mixing of particles, cleavage of chemical bonds and diffusion of reactant atoms followed by the formation of products and nucleation. Clearly, the decomposition processes are faster than syntheses.

Indeed, disproportionation of Al_2SiO_5 into Al_2O_3 and SiO_2 under the action of high-energy shock waves results in the formation of a high-pressure SiO_2 phase with stishovite-type structure.[110, 111] Similar phases are formed under shock compression of $ZnBaGeO_4$,[112] Mg_2SiO_4[113] and $ZrSiO_4$.[114] A high-pressure boron nitride phase (c-BN) was produced by shock-induced disproportionation of $BH_3 \cdot NH_3$.[115] Explosive decomposition of organic compounds mixed with explosives, resulting in the formation of diamond as detonation product was reported.[116, 117] Disproportionation of PbO upon shock compression by high-energy shock waves in a cylindrical ampoule occurs behind the front of the incident shock wave. Propagation of the reflected wave through a mixture is accompanied by separation of the mixture components and accumulation of lead in the Mach region.[118] Therefore, the chemical reaction occurs in the region between the incident and reflected waves and has a duration of 10^{-7}–10^{-6} s.

At high pressure, water possesses the properties of acid. Because of this, metals preceding hydrogen in the electrochemical series should dissolve in this modification of water. Taking into account this fact, we shock compressed a mixture of zinc powder and ice in cylindrical recovery ampoules cooled with liquid nitrogen before explosion using high-power explosives ($D_0 \geqslant 6.2$ km s^{-1}). Analysis of the recovered product revealed the formation of zinc oxide and dihydrogen following the reaction

$$Zn + H_2O = ZnO + H_2.$$

The reaction products cannot result from pyrolysis of water, because the temperature of the ampoule after explosion was only slightly higher than room temperature. Similar reactions proceed with other metals (B, Al, Ga, Ge, Ti, Zr, Nb, Cr, Mo, W, Mn) that dissolve in acids, *i.e.*, the chemical transformation does occur in the high-pressure zone.[119] A similar experiment[120] using a cylindrical ampoule with a large reservoir for expansion and quenching of reaction products (see Fig. 3 *c*) resulted in cubic zirconia (high-pressure phase). The reaction

$$MgCO_3 + Fe \longrightarrow MgO + FeO + C$$

was used for the synthesis of hexagonal diamond (lonsdeilite).[121]

Consider now yet another aspect, which also indicates a shock-wave character of chemical transformations. Thermodynamics operates with positive pressures. As mentioned above, shock compression technique allows production of negative pressures and formation of loose structures.

A shock compression study[122] of Nd_2O_3 revealed the formation of a polymorph called E-phase. According to spectral analysis data, the E-phase also contained SiO_2 (~ 30%). Experiments proved that spall microparticles from the inner surface (mainly from the bottom and to a lesser extent from the walls) of the recovery ampoule served as the source of SiO_2. The density of the E-phase (1.6 g cm^{-3}) is much lower than those of the starting neodymium oxide (7.42 g cm^{-3}) and quartz (2.65 g cm^{-3}). A very small amount of single crystals of this phase was obtained. The crystals had a monoclinic lattice ($a = 7.5$, $b = 8.7$, $c = 10.3$ Å; $\beta = 104°$) and low refractive index ($n_g = 1.57$, $n_m = 1.56$, $n_p = 1.54$), whereas the refractive index of the starting neodymium oxide is 2.10. The E-phase of neodymium oxide is insoluble in acids or alkalis and exhibits a high thermal stability with a reversible change of colour from white to violet. Attempts to obtain this phase under shock compression of Nd_2O_3 + Si, Nd_2O_3 + SiO and Nd_2O_3 + SiO_2 mixtures using various explosives failed. Namely, reactions at any reagent ratios resulted in conventional neodymium silicates of different compositions charaterised by high densities and refractive indices. Apparently, the reactivity of the spall elements is strongly different from the bulk sample reactivity due to an increase in the concentration of ruptured chemical bonds in such species upon spalling from the monolithic body.

Similar results were obtained in a shock compression study of Zr + 2 S mixture, which revealed the formation of ZrS_2 with 'shrinked' unit cell parameters.[123] In a detailed study the product was identified as a solid solution $Zr_{1-x}Fe_xS_2$. Here, the source of iron was also the recovery ampoule (no solid solution is formed when using ampoules with quartz embedments) and the product yield was dependent on the smoothness of the inner surface of the ampoule. The last-mentioned feature means that iron microparticles are spalled from scratches on the inner walls. It is important that no solid solution is formed under shock compression of a mixture of ZrS_2 with iron powder, or by thermal method because the product obtained by shock-induced synthesis decomposes to ZrS_2 and FeS on heating.

When using spall microparticles of elements with equal electronegativities (heat of reaction is zero) as reactants, the thermodynamic situation can change. An example is provided by the reaction

$$Ta + SiO_2 \longrightarrow Ta_2O_5 + Si,$$

which proceeds under shock compression of SiO_2 in tantalum ampoule,[124] being impossible under normal conditions.

The supply of iron spall microparticles from the walls of a cylindrical ampoule to the material compressed is governed by the density of the material (the higher the density the lower the supply) and by the physicochemical processes occurring under shock compression. In particular, an increase in the yield of the dense phase from 45% to 85% during the phase transformation of BN is accompanied by fivefold more intense contamination of the sample with iron from the cylindrical ampoule. Shock compression of PbO, PbF_2 and ZnS accompanied by phase transformations in the compounds causes a twofold increase in the contamination of samples with iron compared to the shock compression of the high-pressure phases that do not undergo any transformations. The contamination of products of the shock-induced syntheses

$$Sn + S \longrightarrow SnS,$$

$$Mn + Te \longrightarrow MnTe,$$

$$Ti + TiO_2 \longrightarrow TiO$$

with iron is two times (MnTe, TiO) or even two orders of magnitude (SnS) higher compared to inert compounds of the same compositions under the same conditions. Correspondingly, shock-induced decomposition of $CdCO_3$ to CdO is accompanied by not only a reduction of temperature and densification but also a decrease in the extent of contamination with iron by an order of magnitude.

An additional argument substantiating the conclusion that solids can undergo chemical transformations under shock is provided by the fact that reactions occur mainly in the axial region of the cylindrical ampoule (Mach region).[91,94] This seemed obvious for long, because the pressure and temperature are maximum in the Mach stem, decrease in the adjacent layer (here, the reaction is only partially completed) and reach minimum values at the walls of the ampoule where no reaction occurs at all. However, it remains unclear why heat released in the shock compressed mixture (extent of chemical conversion is $40 \pm 10\%$ according to experimental data) does not initiate the process in other regions of the sample that contact the hot zone?

The reason for such a behaviour is the high pressure in the Mach zone, which leads to reduction of the temperature of the reacting mixture (see a dome-shaped plot of temperature changes under shock compression of Sn + S mixture in Fig. 8).[125] What processes do occur in the product after unloading if the high pressure underestimates the heat (it can reach zero upon further heating; this is called 'cold synthesis')? Since the compression – expansion cycle is reversible, unloading should be followed by heat release, but why the heat released does not initiate a chemical reaction in the unloaded sample in the region near the axis of the ampoule?

The answer to this question deserves special studies, however to a first approximation one can assume that in the course of unloading at negative pressures the substance arrives at an additional minimum on the potential surface. Probably, this minimum corresponds to an ordered defect or dislocation lattice, because the densities of all substances synthesised by explosion technique were different from the reference values. For instance, heating of shock-synthesised CrTe is accompanied by densification of the material and corresponding exothermic effect at 410 °C. However, we failed not only to complete a transition of the compound to the normal state but even to reach the density of the initial mixture after storage of the sample at 700 °C for 2 h.[126] Therefore, shock-induced synthesis results in compounds that possess new properties. Partial completion of exothermic reactions in recovery ampoules under shock compression can be treated as yet another criterion for occurrence (or absence) of the chemical interaction of solids in the high dynamic pressure zone.

V. Mechanism of ultrafast solid-phase reaction

Experimental facts indicating that solid-phase syntheses can proceed under shock (see above) require a non-trivial explanation. Indeed, conventional diffusion in solids is much slower than that providing the microsecond durations of chemical reactions. Ultrafast atom diffusion in shock compressed materials was explained by several factors. These are a very high concentration of defects, plastic deformation,[127,128] heterogeneous heating of components with different stiffness,[129] reduction of activation energy due to crystal lattice breakdown upon phase transitions [130,131] or melting of one or all reactants.[127] Although all these factors favour a decrease in the activation energy and acceleration of diffusion, they are insufficient to provide an explanation for the mechanism of ultrafast mixing of components in the reacting mixture and separation of reaction products, a threshold-type character of the reaction pressure and other experimental data.

We have hypothesised that ultrafast forced diffusion of mixture components is due to the particle velocity difference between the components under shock compression.[85] This was experimentally proved in a number of studies [132,133] (see also Refs 134 and 135). Indeed, if solid reagents 1 and 2 possess the same mechanical properties, namely, the same shock adiabats and, hence, the particle velocities ($U_1 = U_2$), the motion of the material behind the shock wave front resembles the motion of a chessboard with the same pattern of black and white squares. If differently coloured squares move at different velocities, the velocity difference represents the velocity of forced diffusion ($U_d = U_1 - U_2$), which causes deformation and interdiffusion of the squares. It is important that U_d increases as the pressure increases; this contradicts conventional concepts of retardation of diffusion upon densification. Based on this model, it is possible to immediately determine the mixing time; therefore, the reaction duration can be found as follows

$$\tau \approx \frac{d}{U_d},$$

where d is the grain size. For instance, at $U_d = 1$ km s^{-1} and $d = 0.1$ mm one gets $\tau \approx 10^{-7}$ s.

Strictly speaking, the rate of forced diffusion in a heterogeneous mixture is not equal to $\Delta U_{1,2}$, Here, a fraction of $\Delta U_{1,2}$ should be used with allowance for unloading of the stiff component into the softer body. For most compounds at moderate pressures this fraction is about 0.5 and therefore the characteristic diffusion time (mixing time) should be determined using the relation [80,136]

$$\tau = \frac{2d}{\Delta U_{1,2}}.$$

Knowing the Hugoniot adiabats for Sn, S and Te, one can find with ease that for the Sn + S mixture (particle size 100 μm) the time $\tau = 0.3$ μs corresponds to a pressure of 10 GPa and for the Sn + Te mixture (the same particle size) the time $\tau = 0.8$ μs corresponds to a pressure of 50 GPa. This is consistent with experimental data with allowance for the scatter in the particle size and errors in pressure measurements in the reacting mixture.

How does interdiffusion occur? The most probable model for this process is as follows. Propagation of a shock wave through a heterogeneous mixture of powders is accompanied by fragmentation of grains into blocks of size up to 50 – 100 Å (according to X-ray diffraction data [4]) due to unloading of the stiff material into milder grains. These blocks ('spalled squares') are mixed at a forced diffusion rate. In this case the chemical reaction immediately occurs on the surfaces of the contacting blocks, thus involving from 20% to 40% of the total number of atoms. It is this degree of conversion that is detected by various physical methods (see above). Probably, reactions on the particle surfaces are also favoured by contact melting of grains during shock compression.

The mechanical properties, *e.g.*, U of the reaction product differ from those of the starting components. Due to the particle velocity difference between the reactants and product the particle surfaces are 'cleaned' from the reacting layer, which ensures continuous chemical interaction.

Different stages of solid-phase reactions, namely, grinding before reaction, interdiffusion and, finally, chemical interaction were considered in studies on the microstructure of products of shock compression of powder mixtures M + 2 Si (M = Al, Ti, V, Nb, Ta, Cr, Mo, W, Fe).[94, 137–140] Since the pressure and temperature in cylindrical ampoules rapidly decrease from the axial region to periphery, a transition from the mixture of components to compounds synthesised can be observed using the same sample by analysing its cross-section. With the known law of pressure changes across the section of the cylindrical ampoule one can determine the threshold reaction pressure.[94]

Yet another feature should be noted. The degree of conversion is 100% in the axial region of the cylindrical ampoule, decreases as the shock wave intensity decreases towards the periphery of the cylinder and is zero (no reaction) on the walls of the ampoule, although the decrease in pressure should cause the heat of the reaction to increase. This can be explained as follows: the characteristic time of unloading of a shock compressed body in the laboratory experiments with charges 40 – 60 mm in diameter is $\sim 10^{-6}$ s; the decrease in the dynamic pressure from 100 to 1 GPa means that the duration of the action of the high pressure in each step $\Delta P = 1$ GPa is shortened to $\sim 10^{-8}$ s, which is insufficient for interdiffusion of large reactant particles. Thus, shock-initiated solid-phase chemical reactions proceed with different yields at the same pressure depending on the pressure 'prehistory'. In other words, the results depend on whether the optimum pressure was produced by detonation of a corresponding explosive (here, the duration is $\sim 10^{-6}$ s) or was attained during the drop from a higher level and therefore acts in each step for a much shorter time.

An important feature of shock-initiated reactions is a threshold character of the behaviour of their thermodynamic parameters. Several criteria for the explanation for this phenomenon were proposed. Krüger *et al.* [141] assume that the threshold of the reaction Ni + Si is determined by the critical energy necessary for initiation of the reaction. Iyer *et al.*[142] determined the threshold wave velocity for the reaction Ni + Al; Meyers [143] assumes that the threshold of the onset of the reaction Nb + Si is due to melting of silicon; and Thadhani *et al.*[107] concluded that the threshold of the solid-phase interaction is the ultimate strength of the crystalline particles, *i.e.*, the shock-initiated reaction is a mechanochemical process. According to our model, the pressure corresponding to the onset of the reaction is determined by the time taken by the forced diffusion front (due to the mass velocity difference between components) to travel a distance equal to the particle size.

The thermodynamic and kinetic aspects of shock-initiated solid-phase reactions were considered and the results of numerical modelling of the mechanisms of these reactions were presented.[19]

Theoretical treatment of the possibility of solid-phase detonation as a result of exothermic shock-initiated reaction was reported.[144, 145] Constant shock-wave velocities in the reacting mixtures of zinc and sulfur powders and aluminium and fluoropolymer were observed.[106, 146] Investigations of this phenomenon are of fundamental importance.

VI. Conclusion

There are three promising avenues of research on the chemical transformations under the action of shock waves.

One of them involves improvement of the shock-wave loading techniques, which permits separate variation of thermodynamic parameters of the interacting bodies. For instance, if one reactant is placed in a target and the other reactant is the impactor material, it is possible to increase the chemical potential difference between the reactants that have similar or equal electronegativities (*i.e.*, a low or zero heat of formation) and therefore do not react under normal conditions. An example is provided by B + Sb mixture for which no shock-induced interaction of the components was reported so far.

The second avenue of research in the field of shock-induced synthesis, which has no analogues in traditional chemistry, involves the use of spall microparticles as reactants. In this connection the cumulative effect is of considerable interest. It allows one to generate dense microparticle flows from planar or conical hollownesses in various metals and to control the thermodynamic parameters of reactants by varying the angle of the hollowness, the type of the explosive and the distance to the target.

The third promising field of chemical applications of the shock-wave technique is the synthesis at negative pressures, which results in the formation of loose structures. Macroscopic loose structures can be obtained by shock compression of a mixture of the desired material and explosive in a recovery ampoule. Compression of the ampoule and compaction of the powder are followed by internal detonation and formation of pumice.[147] It is possible to control both the pore concentration and pore topography, which seems to be promising for application in catalysis with allowance for improvement of catalytic activity under shock (see references cited in Ref. 47).

Dynamic-static compression of nanocrystalline powders can also find certain applications. Transition from macroscopic particles to nanoparticles is accompanied by an increase in the elastic modulus by tens of per cent.[148–151] This is due to the surface energy of micropowders. In the bulk crystal the proportion of the surface energy is negligible, but in an array of size 100 Å and a bond length of 2 Å the number of surface atoms is 6×50^2 or 12% of the total number of atoms. The potential energy of the material increase by the same value and, since $E \sim BV$, the elastic modulus will also increase by 12% at the same volume, which is consistent with experimental data. Will attempts to compact diamond nanopowders to monolithic state at the same size be successful, the novel material should be harder than conventional diamond single crystals or polycrystals.

References

1. M D Knudson, J R Asay, C Deeney *J. Appl. Phys.* **97** 073514 (2005)
2. H C Rodean *J. Chem. Phys.* **61** 4848 (1974)
3. P Boogerd, H J Verbeek, M Stuivinga, A C van der Steen, P J van der Put, J Schoonman *J. Appl. Phys.* **78** 5335 (1995)
4. S S Batsanov *Effects of Explosions on Materials* (New York: Springer, 1994)
5. Th S Duffy, Th J Ahrens *J. Appl. Phys.* **76** 835 (1994)
6. A N Afanasenkov, B M Bogomolov, I M Voskoboinikov *Zh. Prikl. Mekhan. Tekhn. Fiz.* (4) 137 (1969) [a]
7. I M Voskoboinikov, O I Voskoboinikova *Khim. Fiz.* **21** (8) 5 (2002) [b]
8. Q Johnson, A C Mitchell, L Evans *Nature (London)* **231** 310 (1971)
9. Q Johnson, A C Mitchell, L Evans *Appl. Phys. Lett.* **21** 29 (1972)
10. L A Egorov, E V Nitochkina, Yu K Orekin *Pis'ma Zh. Eksp. Teor. Fiz.* **16** 8 (1972) [c]
11. F Müller, E Schulze *Z. Naturforsch., A* **33** 918 (1981)
12. A M Podurets, A I Borenboim, V V Pul', R F Trunin *Izv. Akad. Nauk SSSR, Fiz. Zemli* (6) 26 (1989)
13. S S Batsanov *Neorg. Mater.* **38** 1330 (2002) [d]
14. R G McQueen, S P Marsh, J W Taylor, J N Fritz, W J Carter, in *High Velocity Impact Phenomena* (Ed. R Kinslow) (New York: Academic Press, 1970)
15. A L Ruoff *J. Appl. Phys.* **38** 4976 (1967)
16. J Kouam, P Rochegude *J. Mater. Sci. Lett.* **15** 600 (1996)
17. M H Rice, R G McQueen, J M Walsh, in *Solid State Physics* Vol. 6 (Eds F Seitz, D Turnbull) (New York: Academic Press, 1958) p. 62
18. R Boehler, G C Kennedy *J. Phys. Chem. Solids* **41** 1019 (1980)
19. I P H Do, D J Benson *Int. J. Plast.* **17** 641 (2001)

20. Y Noguchi, K Kusaba, K Fukuoka, Y Syono *Geophys. Res. Lett.* **23** 1469 (1996)
21. Y Noguchi, M Uchino, H Hikosaka, T Atou, K Kusaba, K Fukuoka, T Mashimo, Y Syono *J. Phys. Chem. Solids* **60** 509 (1999)
22. T Mashimo, Y Zhang, Y Uemura, T Kobayashi, T Sekine, S M Gavrilkin, S S Batsanov, in *The 5th International Symposium on Impact Engineering, Cambrige, UK, 2004* p. 11
23. T Mashimo, M Uchino, A Nakamura, T Kobayashi, E Takasawa, T Sekine, Y Noguchi, H Hikosaka, K Fukuoka, Y Syono *J. Appl. Phys.* **86** 6710 (1999)
24. J C F Millett, N K Bourne, I P Jones *J. Appl. Phys.* **89** 2566 (2001)
25. D P Dandekar, D C Benfanti *J. Appl. Phys.* **73** 673 (1993)
26. H He, T Sekine, T Kobayashi, H Hirosaki *Phys. Rev. B* **62** 11412 (2001)
27. W J Nellis, F H Ree, M van Thiel, A C Mitchell *J. Chem. Phys.* **75** 3055 (1981)
28. R F Trunin (Ed.) *Svoistva Kondensirovannykh Veshchestv pri Vysokikh Davleniyakh i Temperaturakh* (Properties of Condensed Substances at High Pressures and Temperatures) (Arzamas-16: All-Russian Scientific Research Institute of Experimental Physics, 1992)
29. A Yu Dolgoborodov, I M Voskoboinikov *Khim. Fiz.* **8** 1118 (1989) [b]
30. M V Zhernokletov *Teplofiz. Vys. Temp.* **36** 231 (1998) [e]
31. Ya B Zel'dovich, Yu P Raizer *Fizika Udarnykh Voln i Vysokotemperaturnykh Gidrodinamicheskikh Yavlenii* (The Physics of Shock Waves and High-temperature Hydrodynamic Phenomena) (Moscow: Nauka, 1966)
32. L G Bolkhovitinov, Yu B Khvostov *Nature (London)* **274** 5764 (1978)
33. Yu B Khvostov *Dokl. Akad. Nauk SSSR* **294** 302 (1987) [f]
34. L G Bolkhovitinov, Yu B Khvostov *Fiz. Goren. Vzryva* **24** (5) 119 (1988) [g]
35. L Boshoff-Mostert, H J Viljoen *J. Appl. Phys.* **86** 1245 (1999)
36. J Touvenin *C. R. Acad. Sci.* **258** 3461 (1964)
37. I M Voskoboinikov, A Yu Dolgoborodov, M F Gogulya *Fiz. Goren. Vzryva* **18** (5) 117 (1982) [g]
38. V W Yuan, J D Bowman, D J Funk, G L Morgan, R L Rabie, C E Ragan, J P Quintana, H L Stacy *Phys. Rev. Lett.* **94** 125504 (2005)
39. A Polian, D Vo-Thanh, P Richet *Eur. Lett.* **57** 375 (2002)
40. O Ohtaka, H Fukui, T Kunisada, T Fujisawa, K Funakoshi, W Utsumi, T Irifune, K Kuroda, T Kikegawa *Phys. Rev. B* **63** 174108 (2001)
41. H Ledbetter, A Migliori, J Betts, S Harrington, S El-Khatib *Phys. Rev. B* **71** 172101 (2005)
42. Yu N Ryabinin *Zh. Tekhn. Fiz.* **26** 2661 (1956) [h]
43. D D Gur'ev, Yu A Gordopolov, S S Batsanov *Fiz. Goren. Vzryva* **41** (1) 129 (2005) [g]
44. S S Batsanov *Fiz. Goren. Vzryva* **30** (1) 125 (1994) [g]
45. S S Batsanov, S M Gavrilkin, L I Kopaneva, I I Maksimov, M A Meyers, H C Chen, R Prümmer, E E Seiko, V A Vazyulin *J. Mater. Sci. Lett.* **16** 1625 (1997)
46. G A Adadurov *Usp. Khim.* **55** 555 (1986) [*Russ. Chem. Rev.* **55** 282 (1986)]
47. S S Batsanov *Usp. Khim.* **55** 579 (1986) [*Russ. Chem. Rev.* **55** 297 (1986)]
48. D Bancroft, E L Peterson, S J Minshall *J. Appl. Phys.* **27** 281 (1956)
49. L V Al'tshuler *Usp. Fiz. Nauk* **85** 197 (1965) [*Physics-Uspekhi* **8** 52 (1965)]
50. S B Kormer *Usp. Fiz. Nauk* **94** 641 (1968) [*Physics-Uspekhi* **11** 229 (1968)]
51. S S Batsanov *Zh. Neorg. Khim.* **28** 2723 (1983) [i]
52. B U Alder, in *Solids under Pressure* (New York: McGraw-Hill, 1963) p. 385
53. T Mashimo, K Nakamura, K Tsumoto, Y Zhang, S Ando, H Tonda *J. Phys.: Condens. Matter* **14** 10783 (2002)
54. D Zahn, S Leoni *Z. Kristallogr.* **219** 345 (2004)
55. S S Batsanov, E M Moroz, V P Kuzyutin *Zh. Strukt. Khim.* **11** 156 (1970) [j]
56. S M Gavrilkin, L I Kopaneva, S S Batsanov *Neorg. Mater.* **40** 28 (2004) [d]
57. G A Adadurov, O N Breusov, A N Dremin, V N Drobyshev, A I Lazarev, S V Pershin *Dokl. Akad. Nauk SSSR* **202** 864 (1972) [f]
58. S S Batsanov, E D Ruchkin, L N Travkina, L I Kopaneva, V V Sokolov, A A Kamarzin *Zh. Strukt. Khim.* **16** 698 (1975) [j]
59. S S Batsanov, Yu M Kiselev, L I Kopaneva *Zh. Neorg. Khim.* **25** 1987 (1980) [i]
60. S S Batsanov, V P Bokarev, E V Lazareva *Fiz. Goren. Vzryva* **25** (1) 94 (1989) [g]
61. S S Batsanov, G E Blokhina, A A Deribas *Zh. Strukt. Khim.* **6** 227 (1965) [j]
62. V D Blank, S G Buga, N R Serebryanaya, G A Dubitsky, S N Sulyanov, M Yu Popov, V N Denisov, A N Ivlev, B N Mavrin *Phys. Lett. A* **220** 149 (1996)
63. S S Batsanov *Fiz. Goren. Vzryva* **34** (1) 117 (1998) [g]
64. T Akashi, A Sawaoka, S Saito, M Araki *Jpn. J. Appl. Phys.* **15** 891 (1976)
65. M Sokolowski *J. Cryst. Growth.* **46** 136 (1979)
66. D V Fedoseev, I G Varshavskaya, A V Lavrent'ev, B V Deryagin, V L Bukhovets, V V Matveev, V L Ruzinov, T A Karpukhina *Dokl. Akad. Nauk SSSR* **270** 918 (1983) [f]
67. T Akashi, H-R Pak, A Sawaoka *J. Mater. Sci.* **21** 4060 (1986)
68. H Nameki, T Sekine, T Kobayashi *J. Mater. Sci. Lett.* **15** 1492 (1996)
69. M Gagnier, H Szwarc, A Ronez *J. Mater. Sci.* **35** 3003 (2000)
70. S S Batsanov *NATO Science Series. II Mathematics, Physics and Chemistry* Vol. 140 (Dordrecht: Kluwer, 2004) p. 353
71. N N Shevtsova, I N Temnitskii, S S Batsanov *Zh. Neorg. Khim.* **32** 2596 (1987) [i]
72. G V Dorogova, L I Kopaneva, S S Batsanov *Fiz. Khim. Obrabot. Mater.* (4) 140 (1988)
73. N M Kuznetsov, in *Udarnye Volny i Ekstremal'noe Sostoyanie Veshchestva* (Shock Waves and Extremal State of Substance) (Eds V E Fortov, L V Al'tshuler, R F Trunin, A I Funtikov) (Moscow: Nauka, 2000) p. 174
74. S S Batsanov, G S Doronin, A A Nerchenko, V V Roman'kov, A E Strelyaev, V P Stupnikov *Inzh.-Fiz. Zh.* **24** 354 (1973) [k]
75. R B Heimann, J Kleimann, N M Salansky *J. Cryst. Growth* **67** 213 (1984)
76. S S Batsanov *Fiz. Goren. Vzryva* **32** (1) 115 (1996) [g]
77. H Hornig, J Kury, R Simpson, F Helm, W von Holle, in *Proceedings of the 11th International Pyrotechnics Seminar, Vail, CO, 1986* p. 699
78. M B Boslough *Chem. Phys. Lett.* **160** 618 (1989)
79. M B Boslough *J. Chem. Phys.* **92** 1839 (1990)
80. S S Batsanov, M F Gogulya, M A Brazhnikov, G V Simakov, I I Maksimov *Fiz. Goren. Vzryva* **30** (3) 107 (1994) [g]
81. S S Batsanov, M F Gogulya, M A Brazhnikov, E V Lazareva, G S Doronin, S V Klochkov, M B Banshchikova, A V Fedorov, G V Simakov *Khim. Fiz.* **10** 1699 (1991) [b]
82. M F Gogulya, I M Voskoboinikov, A Yu Dolgoborodov, N S Dorokhov, M A Brazhnikov *Khim. Fiz.* **10** 420 (1991) [b]
83. M F Gogulya, I M Voskoboinikov, A Yu Dolgoborodov, N S Dorokhov, M A Brazhnikov *Khim. Fiz.* **11** 244 (1992) [b]
84. M F Gogulya, M A Brazhnikov *Khim. Fiz.* **13** (11) 88 (1994) [b]
85. S S Batsanov, G S Doronin, S V Klochkov, A I Teut *Fiz. Goren. Vzryva* **22** (6) 135 (1986) [g]
86. A Yu Gordopolov, Yu A Gordopolov, V M Fedorov, R M Shekhverdiev, in *XII Simpozium po Goreniyu i Vzryvu, Chernogolovka, 2000* (The XIIth Symposium on Combustion and Explosion, Chernogolovka, 2000)
87. X Xu, N N Thadhani *J. Appl. Phys.* **96** 2000 (2004)
88. M Uchino, T Mashimo, M Kodama, T Kobayashi, E Takasawa, T Sekine, Y Noguchi, H Hikosaka, K Fukuoka, Y Syono, T Kondo, T Yagi *J. Phys. Chem. Solids* **60** 827 (1999)
89. I Barin *Thermodynamical Data of Pure Substances* (3rd Ed.) (Weinheim: VCH, 1995)
90. A Grzechnik, P Simon *J. Phys.: Condens Matt.* **11** 2337 (1999)
91. K S Vandersall, N N Thadhani *J. Appl. Phys.* **94** 1575 (2003)
92. K S Vandersall, N N Thadhani *Metall. Mater. Trans. A* **34** 15 (2003)
93. T Vreeland *Scr. Mater.* **38** 337 (1998)

94. S S Batsanov, S M Gavrilkin, F D Markis, M A Marquis *Zh. Neorg. Khim.* **42** 110 (1997) [i]
95. M A Podurets, G V Simakov, R F Trunin *Izv. Akad. Nauk SSSR, Fiz. Zemli* (4) 28 (1988)
96. I M Voskoboinikov *Khim. Fiz.* **17** 132 (1998) [b]
97. R D Dick *J. Chem. Phys.* **52** 6021 (1970)
98. I M Voskoboinikov *Khim. Fiz.* **10** 672 (1991) [b]
99. R F Trunin, M V Zhernokletov, N F Kuznetsov *Khim. Fiz.* **11** 424 (1992) [b]
100. I M Voskoboinikov *Fiz. Goren. Vzryva* **39** (2) 105 (2003) [g]
101. C E Morris, J N Fritz, R G McQueen *J. Chem. Phys.* **80** 5203 (1984)
102. M Yoshida, N N Thadhani, in *Shock Compression in Condensed Matter — 1991* (Eds S C Schmidt, R D Dick, I W Forbes, D G Tasker) (New York: Elsevier, 1992) p. 585
103. I M Voskoboinikov, A Yu Dolgoborodov, in *Detonatsiya i Udarnye Volny. Materialy 8 Vsesoyuznogo Simpoziuma po Goreniyu i Vzryvu, Tashkent 1986* (Detonation and Shock Waves. Proceeding of the 8th All-Union Symposium on Combustion and Explosion, Tashkent 1986) p. 9
104. A Yu Dolgoborodov, I M Voskoboinikov, M F Gogulya, I K Tolstov, in *V Vsesoyuznoe Soveshchanie po Detonatsii, Krasnoyarsk, 1991* (The Vth All-Union Meeting on Detonation, Krasnoyarsk, 1991) p. 140
105. D L Gur'ev, Yu A Gordopolov, S S Batsanov *Fiz. Goren. Vzryva* **42** (1) 130 (2006) [g]
106. D L Guriev, Y A Gordopolov, S S Batsanov, A G Merzhanov, V E Fortov *Appl. Phys. Lett.* **88** 024102 (2006)
107. N N Thadhani, R A Graham, T Royal, E Dunbar, M U Anderson, G T Holman *J. Appl. Phys.* **82** 1113 (1997)
108. S S Batsanov, E E Andrianova, E V Lazareva *Khim. Fiz.* **8** 1435 (1989) [b]
109. S S Batsanov, S M Gavrilkin, A Yu Gordopolov, Yu A Gordopolov *Fiz. Goren. Vzryva* **40** (5) 118 (2004) [g]
110. H Schneider, W Klee, U Hornemann *J. Mater. Sci.* **15** 154 (1980)
111. H Schneider, U Hornemann *J. Mater. Sci.* **16** 45 (1981)
112. H Takei, Y Syono, T Goto, M Kikuchi *Phys. Chem. Miner.* **10** 16 (1983)
113. J Watt, T J Ahrens *J. Geophys. Res. B* **88** 9500 (1983)
114. K Kusaba, Y Syono, M Kikuchi, K Fukuoka *Earth Planet. Sci. Lett.* **72** 433 (1985)
115. R Liepins, K P Staudhammer, K Johnson, M Thomson *Matter. Lett.* **7** 44 (1988)
116. N R Greiner, D Fillips, J Johnson *Nature (London)* **333** 440 (1988)
117. A I Lyamkin, E A Petrov, A P Ershov, G V Sakovich, A M Staver, V M Titov *Dokl. Akad. Nauk SSSR* **302** 611 (1988) [f]
118. S M Gavrilkin, Yu E Zaichikov, S S Batsanov *Fiz. Goren. Vzryva* **36** (4) 131 (2000) [g]
119. S S Batsanov, E V Lazareva, L I Kopaneva *Khim. Vys. Energ.* **16** 184 (1982) [l]
120. S S Batsanov, D L Gur'ev, L I Kopaneva *Fiz. Goren. Vzryva* **24** (4) 132 (1988) [g]
121. T Sekine *Naturwissenschaften* **75** 462 (1988)
122. S S Batsanov, A A Deribas *Fiz. Goren. Vzryva* **1** 103 (1965) [g]
123. S S Batsanov, L I Kopaneva, E V Lazareva, V N Gavryushin, V N Isaev, P V Porokhov *Fiz. Goren. Vzryva* **26** (5) 129 (1990) [g]
124. M Kikuchi, Y Syono, K Fukuoka, K Hiraga *J. Mater. Sci. Lett.* **6** 97 (1987)
125. S S Batsanov *Fiz. Goren. Vzryva* **42** (2) 128 (2006) [g]
126. S S Batsanov, E S Zolotova *Dokl. Akad. Nauk SSSR* **180** 93 (1968) [f]
127. A N Dremin, O N Breusov *Usp. Khim.* **37** 898 (1968) [*Russ. Chem. Rev.* **37** 392 (1968)]
128. S Raikes, Th Ahrens *Geophys. Royal Astron. Soc.* **58** 717 (1979)
129. S S Batsanov, in *Detonatsiya. Kriticheskie Yavleniya. Fiziko-khimicheskie Prevrashcheniya v Udarnykh Volnakh* (Detonation. Critical Phenomena. Physicochemical Transformations in Shock Waves) (Chernogolovka: Branch of Institute of Chemical Physics, Academy of Sciences of the USSR, 1978) p. 126
130. S S Batsanov *Zh. Neorg. Khim.* **27** 1903 (1982) [i]
131. L-G Liu *Earh Planet. Sci. Lett.* **71** 104 (1984)
132. N A Kostyukov *Zh. Prikl. Mekhan. Tekhn. Fiz.* (3) 54 (1988) [a]
133. S S Batsanov, I I Maksimov *Khim. Fiz.* **9** 1274 (1991) [b]
134. A Yu Dolgoborodov, I M Voskoboinikov, I K Tolstov, A V Sudarikov *Fiz. Goren. Vzryva* **28** (3) 106 (1992) [g]
135. Y Horie, in *Metallurgical and Materials Applications of Shock-Wave and High-Strain-Rate Phenomena* (Eds L E.Murr, K P Staudhammer, M A Meyers) (New York: Elsevier, 1995) p. 603
136. S S Batsanov *Mater. Sci. Eng. A* **210** 57 (1996)
137. K S Vecchio, L-H Yu, M A Meyers *Acta Metall. Mater.* **42** 701 (1994)
138. M A Meyers, L-H Yu, K S Vecchio *Acta Metall. Mater.* **42** 715 (1994)
139. S S Batsanov, F D S Marquis, M A Meyers, in *Metallurgical and Materials Applications of Shock-Wave and High-Strain-Rate Phenomena* (Eds L E.Murr, K P Staudhammer, M A Meyers) (New York: Elsevier, 1995) p. 715
140. M A Meyers, S S Batsanov, S M Gavrilkin, H C Chen, J C LaSalvia, F D S Marquis *Mater. Sci. Eng. A* **201** 150 (1995)
141. B R Krüger, A H Mutz, T J Vreeland *J. Appl. Phys.* **70** 5362 (1991)
142. K R Iyer, L S Bennet, F Y Sorrell, Y Horie, in *High Pressure Science and Technology — 1993* (New York: AIP, 1993) p. 1337
143. M A Meyers *Dynamic Behaviours of Materials* (New York: Wiley, 1994)
144. L S Bennett, Y Horie *Shock Waves* **4** 127 (1994)
145. Yu A Gordopolov, V S Trofimov, A G Merzhanov *Dokl. Akad. Nauk* **341** 327 (1995) [f]
146. A Yu Dolgoborodov, M N Makhov, I V Kolbanev, A I Streletskii, V E Fortov *Pis'ma Zh. Eks. Teor. Fiz.* **81** 311 (2005) [c]
147. S S Batsanov, V P Bokarev, I I Maksimov, V A Tumanov *Fiz. Goren. Vzryva* **29** (5) 102 (1993) [g]
148. J Z Jiang, J S Olsen, L Gerward, S Morup *Europhys. Lett.* **44** 620 (1998)
149. Z Wang, S K Saxena, V Pischedda, H P Liermann, C S Zha *Phys. Rev. B* **64** 012102 (2001)
150. Z Wang,Y Zhao, D Schiferl, C S Zha, R T Downs, T Sekine *Appl. Phys. Lett.* **83** 3174 (2003)
151. B Kiefer, S R Shieh, Th S Duffy, T Sekine *Phys. Rev. B* **72** 014102 (2005)

[a] — *J. App. Mech. Tech. Phys. (Engl. Transl.)*
[b] — *Chem. Phys. Rep. (Engl. Transl.)*
[c] — *J. Exp. Theor. Phys. Lett. (Engl. Transl.)*
[d] — *Inorg. Mater. (Eng. Transl.)*
[e] — *High Temp. (Engl. Transl.)*
[f] — *Dokl. Phys. (Engl. Transl.)*
[g] — *Combust. Explos. Shock Waves (Engl. Transl.)*
[h] —*Thech. Phys. (Engl. Transl.)*
[i] — *Russ. J. Inorg. Chem. (Engl. Transl.)*
[j] — *J. Struct. Chem. (Engl. Transl.)*
[k] — *J. Eng. Phys. Thermophys. (Engl. Transl.)*
[l] — *High Energy Chem. (Engl. Transl.)*